MASTER'S THESIS

Dry Water

Jakob Bomhard

Master of Science
Civil Engineering

Luleå University of Technology
Department of Civil, Environmental and Natural Resources Engineering

LULEÅ UNIVERSITY OF TECHNOLOGY

Dry Water

Jakob Bomhard

Division of Architecture and Water
Department of Civil, Environmental and Natural Resources Engineering
Luleå University of Technology
SE-971 87 LULEÅ
SWEDEN

Diploma thesis

Foreword

This Master Thesis is the final result of my regular university education and will be accepted as a Diploma Thesis in my home university in Augsburg/Germany. The work was carried out in the spring semester 2011 at the Department of Civil, Environmental and Natural Resources Engineering at Luleå University of Technology.

During the project I had contact to many people giving me grateful advices, support, help and encouragement for which I would like to thank all these people. First of all of course my supervisor Professor Bo Nordell without him I would have never started this exciting project. His great enthusiasm for the topic aroused my interest studying this largely unknown subject. I am also grateful for his tips and practical advices during my laboratory work as well as contacting me to other helpful people.

Special thanks goes to Wacker Chemie AG, who provided a free sample of Fumed Silica nanoparticles that allowed me to carry out experiments on dry water.

I would like to thank Tommy Wikström, Ulla-Brit Uvemo and Desiree Nordmark for providing a great help in the laboratory. Thank you also to Thomas Forsberg and Roger Lindfors for the technical advices, Roland Pusch for providing his measuring instruments as well as Maine Ranheimer for her help with technical devices.

I also want to thank ClimateWell AB, Stockholm, for the initial advices for preparing dry water, Nils Svanljung for offering attractive help during my project and all people who I should have forgotten to mention.

It is my sincere hope that the knowledge gained during this project will be a small contribution to give dry water a place in the modern scramble of sustainable energy material.

Abstract

Dry water is a solidified, powdered form of water which has the appearance of icing sugar. It contains up to 98 % of water by weight and yet is a dry powder. Each particulate consists of a small water droplet surrounded by a network of highly hydrophobic fumed silica particles. The coating, kept together due to the cohesion between the silica particles, is strong enough to avoid coalescence of the water droplets.

Discovered in the 1960s, scientists have not been devoted any attention to dry water for almost four decades. But it was rediscovered in 2006 in order to study its structure and to exploit it for potential applications. Within the scope of this study, dry water was prepared and more various fundamental characteristics were investigated.

It showed that dry water can be easily prepared by a simple mixing process. It is characterized by good flow properties, a considerable decrease of density compared to bulk water and therefore a large air content. Microscopic droplets lead to a large water/air interface with silica particles between. When cooled to minus temperatures dry water shows significant deviations concerning the freezing point and the evaporation rate and still is flowable.

Attributed to its large water/air interface, the substance has great potential to store gases in an effective and save way in form of gas hydrates. Also the kinetics of chemical reactions can be increased by using chemical reactants instead of water. Dry acids or dry emulsions can be prepared in the same way, offering a safer way for handling and transporting hazardous liquids. But also the use as a cooling agent even at minus temperatures could be a suitable application.

Zusammenfassung

Trockenes Wasser ist ein Pulver, das an Puderzucker erinnert. Es besteht aus bis zu 98 % Wasser und ist dennoch ein trockenes Pulver. Jedes Pulverteilchen enthält einen mikroskopisch kleinen Wassertropfen, der von modifizierten, hoch hydrophoben Siliziumpartikeln umhüllt ist. Diese Hülle wird durch die Kohäsionskräfte der Siliziumpartikel zusammengehalten und verhindert dadurch das Zusammenfließen der Wassertropfen.

Entdeckt wurde es bereits in den 1960er Jahren, fand aber zunächst keine Beachtung. Erst 2006 wurde die Substanz von Wissenschaftlern näher untersucht, um sie für mögliche Anwendungen nutzbar zu machen.

Im Rahmen dieser Arbeit wurde trockenes Wasser hergestellt und weitere grundsätzliche Eigenschaften der Substanz bestimmt.

Trockenes Wasser lässt sich sehr leicht in einem einfachen Mischverfahren herstellen. Das dadurch entstandene Pulver zeichnet sich durch ein gutes Fließverhalten aus und hat durch die im Vergleich zu normalen Wasser reduzierte Dichte einen großen Luftgehalt. Die kleinen Wassertropfen im Pulver führen zu einer hohen Wasseroberfläche. Wird trockenes Wasser Minustemperaturen ausgesetzt, so zeigen sich im Vergleich zu flüssigen Wasser Abweichungen im Gefrierpunkt und bei der Verdunstungsrate. Es bleibt dennoch ein fließfähiges Pulver.

Die Substanz hat aufgrund der großen Grenzfläche zwischen Wasser und Luft ein großes Potenzial zum Speichern von Gasen in Form von Gashydraten. Ebenso kann durch die erhöhte Oberfläche die Geschwindigkeit chemischer Reaktionen erhöht werden. Das Prinzip der Trockenwasserherstellung kann auch an Säuren oder Emulsionen angewendet werden, wodurch eine sicherere Handhabung gefährlicher Substanzen erreicht werden kann. Denkbar ist aber auch der Einsatz von trockenem Wasser als Kühlmittel bei Minustemperaturen.

Table of content

1. Introduction

"Dry water could make a big splash commercially". This is the headline of a report published by American Chemical Society in August 2010. It alludes to the fascinating substance which has been started attracting attention by scientists in the last years and is nevertheless quite unknown.

Dry water - it sounds like a contradiction. It is a powdery substance resembling confectioners' sugar but still consists of up to 98 % water and yet is a dry powder. Each powder particle contains a water droplet surrounded by submicroscopic silica particles (Figure 1). The silica coating prevents the water droplets from combining and turning back into a liquid. The result is a fine powder which is stable and remains flowable over a wide temperature range, even when cooled to minus temperatures.

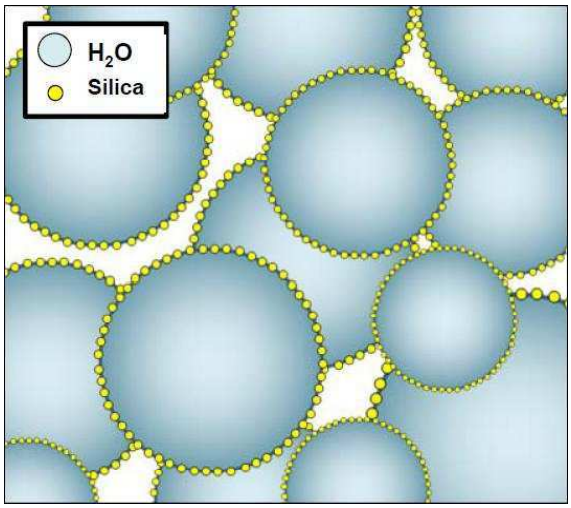

Figure 1: *Water droplets coated by silica particles*

Discovered in 1964, it was first described by D. Schutte in a US-patent 1968 as "predominantly aqueous compositions in a fluffy powdery form" ((Schutte, D. Schmitz, F.-T. & Brünner, H., 1968)). The patent assignee was a pharmaceutical company named DEGUSSA which had seen the invention as a potential component for cosmetics.

But since it was patented, dry water has attracted a surprisingly small amount of published research. Only in the recent years, scientists have rediscovered and studied the substance further in order to expand its potential.

Small coated water droplets enabling a stable formation will lead to more differing properties compared to bulk water. A high water/air interface or flowability at minus temperature could make the substance interesting for miscellaneous technical applications. Dry water as a coolant in cold areas or a solvent for gases might be conceivable applications deserving a detailed study of this substance.

2. Objectives

In order to explain the colloidal basis for the formation process, scientists have started to investigate dry water in the recent years (Binks & Murakami, 2006). More investigations followed studying the exploitation of specific characteristics for potential technical applications (Binks & Murakami, 2006; B. O. Carter, 2010; Wang, Bray, Adams, & Cooper, 2008).

But still the substance is not well known yet in the modern world of science. Thus, the objective of this work was the study of the basics by preparing dry water and determining fundamental properties. By comparing it with bulk water, typical characteristics have been substantiated. The aim was also to find suggestions of more possible technical uses in order to expand its range of applications.

May this information help the scale-up of the knowledge to pre-industrial or industrial units and rise dry water to a sustainable energy material.

3. The component parts

In the following section it will be focused on generally information about the component parts of dry water, water and silica particles. Since a lot of characteristics of its components have a significant influence on dry water properties, the most important ones will be explained in more detail.

3.1. Water

Water is one of the most interesting elements in the nature. Compared to similar substances, it shows many unusual and unexpected properties, without them it would not have been possible a life as we know it. Enumerating all its wide variety of special characteristics and utilities would be redundancy. But nevertheless, the fundamental structure of water as well as some characteristics having a significant influence on dry water must be explained.

Water molecule as a dipole

The geometry of a water molecule H_2O describes a bent structure of two positive charged hydrogen atoms with a negative charged oxygen atom between them (Figure 2a). Its charge difference and asymmetrical charge distribution gives a strong polar trait to the molecule. This dipole character ensures that water molecules can strongly attract to each other by forming hydrogen bonds.

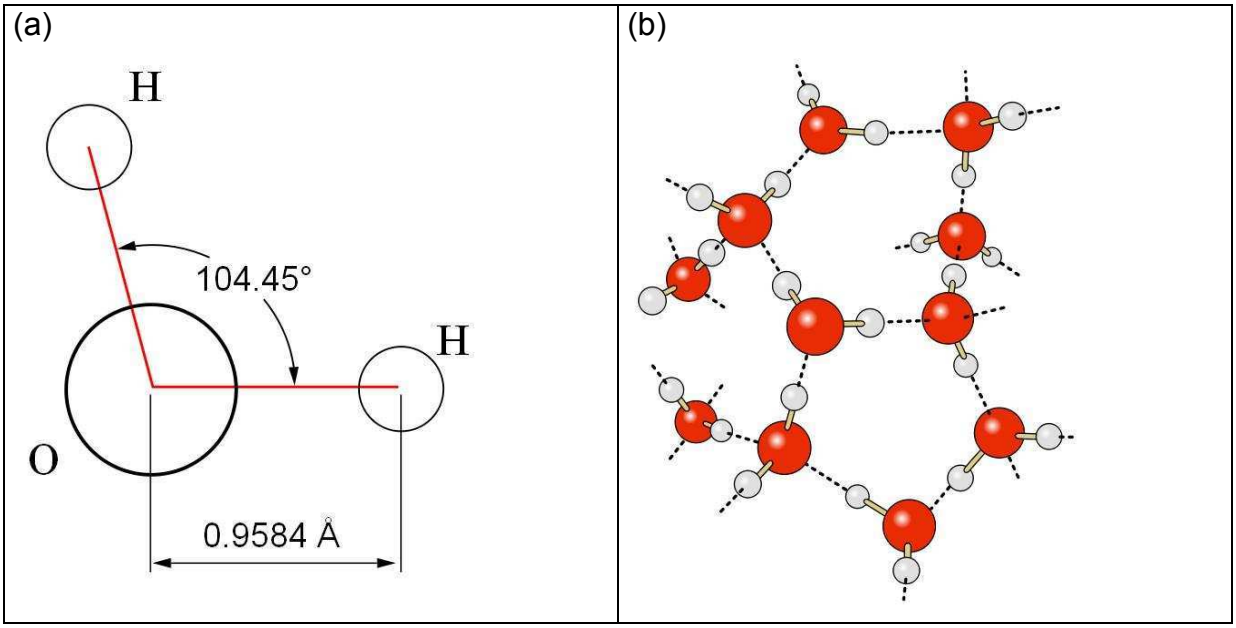

Figure 2: *(a) Water molecule and (b) hydrogen bondings*

The typical properties making water to a unique substance are attributed to these hydrogen bridge bonds where the oxygen with a partial negative charge attracts to the partial positive charge on the hydrogen of another molecule (Figure 2b). The most important properties are:

- The melting and boiling point of 0 °C and 100 °C respectively are unusual high compared to similar substances
- Water has a high specific heat capacity of 4,18 $\frac{kJ}{kgK}$ (at 20 °C), enabling a great temperature regulator
- The large heat of fusion and vaporization of 333,5 $\frac{kJ}{kg}$ and 2256,5 $\frac{kJ}{kg}$ (at 1013,25 hPa) is just like the heat capacity the second highest of all liquids.
- At 3,98 °C water reaches its maximum density affecting the temperature stratification and circulation in lakes and seas
- Ice at 0 °C is approximately 9 % less dense than liquid water at 0 °C, consequently it floats on water

- A high surface tension due to strong hydrogen bonds plays a key role for the drop formation

Water is rarely pure since it is an excellent solvent for ionic and polar substances like acids, alcohols and salts. Also some gases like oxygen, carbon dioxide and methane can dissolve in water making the oceans to a huge sink for carbon dioxide. Under high pressure and low temperatures gas molecules can agglomerate forming hydrates as an ice-like crystalline solid mixture of natural gas molecules and surrounding water molecules (Demirbas, 2010).

Is the water very pure without seed crystals or nucleus, it can be supercooled to minus temperatures without freezing (Bigg, 1953). The volume as well as the rate of cooling plays an important role. Small water droplets with a diameter of 100 µm can have a mean freezing temperature of -30 °C (Figure 3). In nature supercooled water droplets can be found for instance in cold clouds.

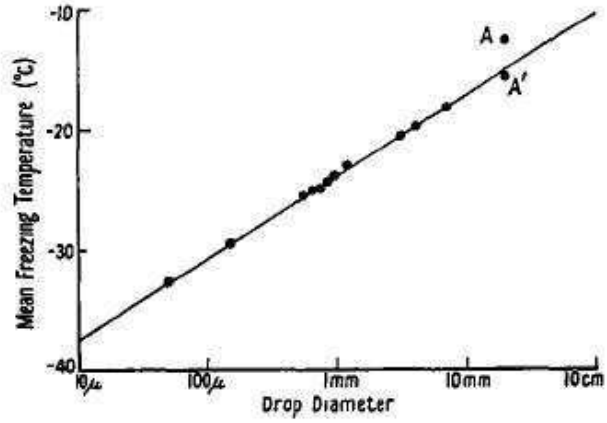

Figure 3: *Mean freezing temperature vs. drop diameter; (Bigg, 1953)*

Another phenomenon which can be observed in nature is the mass loss of freezing water. During the change of state, latent heat is released causing sublimation without a change in temperature. The mass reduction is typically 2,5 - 3 % of the emerged ice mass, depending on factors like air humidity or wind velocity (Skogsberg, 2005). In the spring with repeated freezing and thawing periods, the mass loss can accumulate to a significant ice and snow decrease.

3.2. Pyrogenic silica

Apart usual water, dry water consists of modified nanoparticles of highly pure silica dioxide. Attributed to the nanoscaled size and a special treatment making them intensely hydrophobic, the particles have particular characteristics enabling a water droplet encapsulation. It is also known as fumed silica since it is produced in a flame. It has the appearance of a light white powder (Figure 4).

Figure 4: *Pyrogenic silica particles*

3.2.1. Nanoparticles

The term "Nanoparticle" refers to the size of 1 to 100 nm which particles from both anthropogenic and natural origin have. Having been known for centuries from volcanic eruption, forest fire or salt aerosols at seashores, specially manufactured nanoparticles have entered the industrial sector over the last years. Thereby the special features primary due to the small size and large surface area are utilized for a large range of applications (Dr. Mathias Schulenburg, 2008; Hannink & Hill, 2006; LfU BW, Juli 2007; M. Sc. Hicham Ahmad Fadel, 2005).

3.2.2. Silicon dioxide

Silicon dioxide (SiO_2) comprises a substantial portion of the Earth's surface in form of quartz. It is known for its hardness and chemical resistance. SiO_2 crystallizes in a number of distinct polymorphs but also occurs in amorphous forms and finds many different technical applications. The quantitatively largest amount of SiO_2 is used in glasses in addition to frequency control, microelectronics, chemical processing, ceramics and corrosion control (Devine, 2000).

3.2.3. Production of pyrogenic silica particles

As the name suggests, pyrogenic silica is prepared in a hot gaseous environment by flame hydrolysis at over 1000 °C. The starting products are volatile chlorosilanes, which get introduced into an oxyhydrogen flame, producing high-viscosity SiO_2 primary particles of 5 - 50 nm in size. In the flame, the primary particles fuse together permanently forming larger units, the aggregates with a size of 100 - 1000 nm. An aggregate is the smallest particulate in which fumed silica can be dispersed. On cooling, they mechanically entangle by weak interaction forces forming agglomerates, which are about 1- 250 micrometers in size (Wacker Chemie AG, 2009). The size of aggregates and agglomerates can be influenced by different parameters, depending on the desired end-product. Large agglomerates can be easily broken by sonication (L. Forny, Pezron, Saleh, Guigon, & Komunjer, 2007).

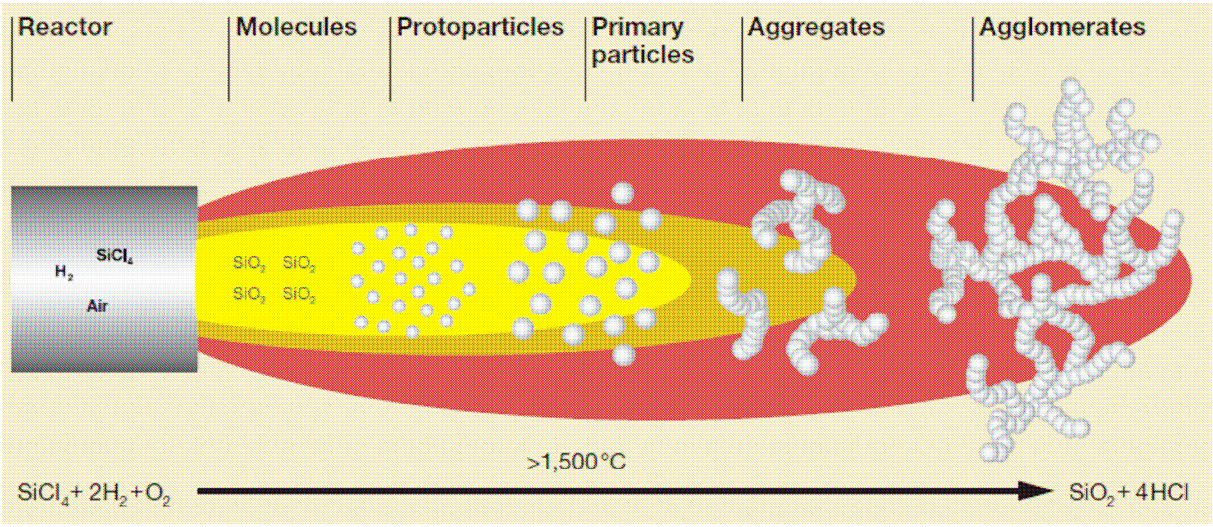

Figure 5: *Pyrogenic silica formation in a flame; www.wacker.com*

After the hydrolysis, the agglomerates have hydrophilic properties. To achieve a hydrophobic surface, they react with methyl chlorosilanes. This treatment ensures a water-repellent effect eliminating the moisture absorption of the silica.

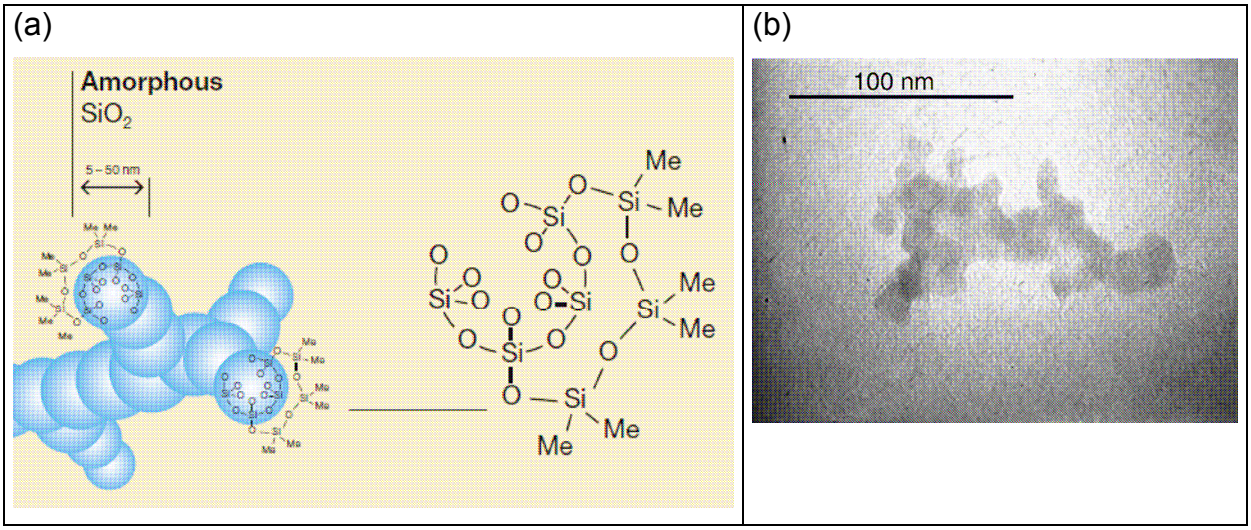

Figure 6: *(a) fumed silica particle with modified, hydrophobic surface; www.wacker.com; (b) TEM observation of a fumed silica aggregate (L. Forny et al., 2007)*

Major global producers of pyrogenic silica are Evonik (Germany), Cabot (United States) and Wacker Chemie AG (Germany).

3.2.4. Properties

The characteristics of the product that has been created is the open-structured and therefore mesoporous formation with pore diameters between 2 nm and 50 nm (Roberts, 1997). The particles have a very high specific surface area due to the small diameters of the primary particles. They are quite chemically resistant, virtually not soluble in water and almost not in acid (except hydrofluoric acid). The particles have an extremely low thermal expansion with a high resistance against fast temperature changes. They also have a high transparence for ultraviolet light and a high fire resistance (refractoriness) (Günther, 2008).

Referring to Wacker Chemie, fumed silica particles are not known to have harmful effects on humans. In animal experiments there are no indications of reproductive effects. They are not carcinogenic (Group 3 “not classifiable as to its carcinogenicity to humans” (WHO, 2010)) and do not cause silicosis.

The degree of hydrophobicity depends on the specific surface area, the substitution rate (carbon content) and the chemical hydrophobicity of the substituted group (L. Forny et al., 2007). The residual silanol content in relation to the hydrophilic silica is a comparative value to classify the particles. Hydrophobic silica particles have a residual silanol content of less than 50 % (Binks & Murakami, 2006).

3.2.5. Applications

Synthetic manufactured silicon dioxide in the form of particles became unnoticedly important in everyday life. Since it is a non-toxic substance, it has applications in many different products.

Pharmaceutical articles as well as cosmetic products contain fumed silica as a carrier for actives or tableting aids. It is used in the food production as the food additive E551, for beer fining or as a defoamer component. Even in the toothpaste it has an application as a hard abrasive to remove tooth plaque.

In volume, the main application of SiO_2 - particles is the filling agent for plastics and sealants, especially in rubber goods. Wacker Chemie produces the particles mainly as thickening agent, reinforcement, flow enhancer and processing aid for the plastics and pharmaceutical industry.

4. Previous studies on dry water

Not many researches have dealt with the substance since its potential applications are not obvious immediately. Laurent Forny and his co-workers at Université de Technologie de Compiègne, France, started investigating the substance in order to understand the occurrence of dry water formation (L. Forny, 2009; L. Forny et al., 2007). More published researches were only carried out in England from scientists at Hull University and Liverpool University, examining potential applications (Binks & Murakami, 2006; B. O. Carter, Wang, Adams, & Cooper, 2010).

4.1. Preparation techniques

Dry water can be prepared easily by mixing the fumed silica particles with water at high rotational speed or alternatively in a modified low shear mixing process.

A commercial blender with a rotating knife blade causing high shear rates is suitable to prepare small amounts of dry water. A study by Forny and co-workers showed that a minimum rotational speed of 12000 rpm for at least 30 s is required to get a good powder formation (L. Forny et al., 2007). The strong stirring conditions are necessary to disperse the bulk water into individual droplets which can be coated with the silica particles. At a lower mixing process the liquid and solid phase would remain separated due to the strong hydrophobic particles.

In order to get a powder formation at a low rotational mixing speed, the water must be atomized before getting in contact with the particles. Small water droplets with a diameter of around 80 µm can be wrapped by stirring the silica particles at a speed of 155 rpm. With the low energy mixing process it is possible to produce dry water powder in large quantities.

4.2. Powder characterization

Since dry water consists of water droplets surrounded by a network of silica particles, it is effectively a water-in-air emulsion (B. O. Carter et al., 2010). The characteristics like droplet size and water uptake capacity strongly depend on the type of silica particles which are used but also the type of preparation plays a role.

The highest water content of 98 % in weight can be achieved with a high speed blender and highly hydrophobic silica particles. (L. Forny, 2009). The dry water particles have various shapes from spherical to oblong, whereas the smaller the size is the more spherical are the shapes (Figure 7b). The diameter varies in a range of approximately 20 to 400 µm. Particle size analysis have shown a mean size diameter $d_v(50)$ of around 120 µm (Figure 7a). But even smaller primary droplet sizes of <20 µm can be reached by varying the speed of mixing (Wang et al., 2008).

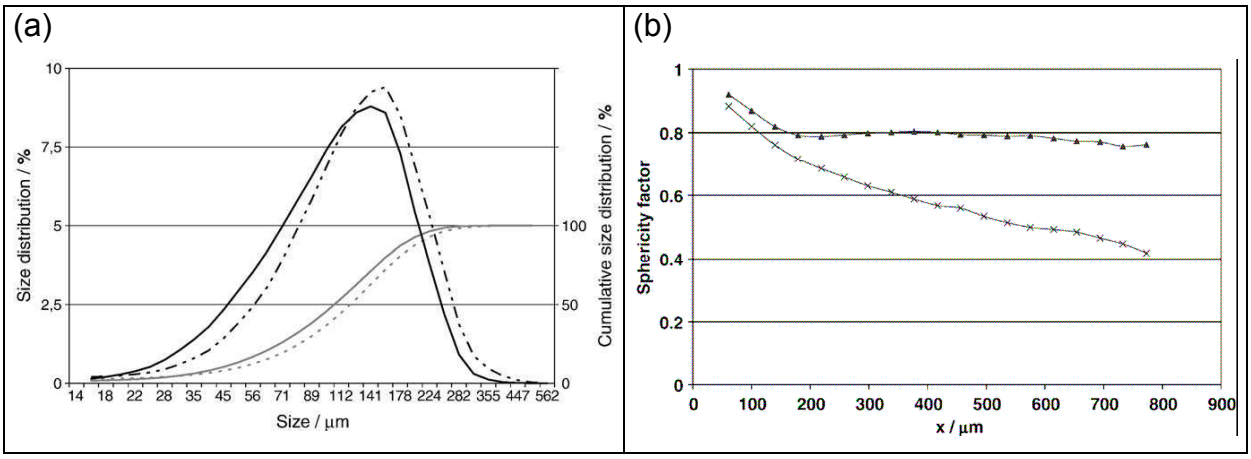

Figure 7: *(a) Size distribution (% in volume) of DW using different hydrophobic silica particle (continuous line = more hydrophobic), (L. Forny et al., 2007); (b) sphericity factor as a function of particle size produced in low shear (▲) and high shear (x) mixing process, (L. Forny, 2009).*

The powder reveals a good flowability since it can be poured easily through a small funnel. A study by Forny has shown a compressibility of minimum 20 % and an angle of repose of at least 44°. Due to these parameters indicating the flow characteristics, dry water has as passable flowability (L. Forny et al., 2007).

Referring to the density of bulk water, the value for dry water powder is decreased by a factor of 2,5 (Binks & Murakami, 2006). This corresponds to a level of 400 kg/m³. Compared to the density of water of around 1000 kg/m³, it indicates a considerable content of air between the dry water particles. Also a high amount of small droplets lead to a highly distributed water-air interface formed across the surface of the dry water droplets. More precise analyses will be carried out in the experimental part.

4.3. Coating of water droplets

The good flowability of dry water powder suggests individual droplets with no water bridges between them. Since the dry water powder remains in its state after preparation, the coating of silica particles is strong enough to prevent coalescence of the droplets. This is reached by a strong interaction of the fumed silica.

Figure 8a shows the particulate shell of a broken dry water particle revealing the chamber for the water droplet inside the silica network. It was achieved by sublimating frozen water under controlled temperature and pressure. The part of a thin coating in Figure 8b were made visible with transmission electron microscopy (TEM) using freeze fracture method (L. Forny et al., 2007). It shows a clear interface between the water droplet and the silica network. The particles forming the coating interact with the surface of the water droplets without being immersed into the liquid.

(a) (b)

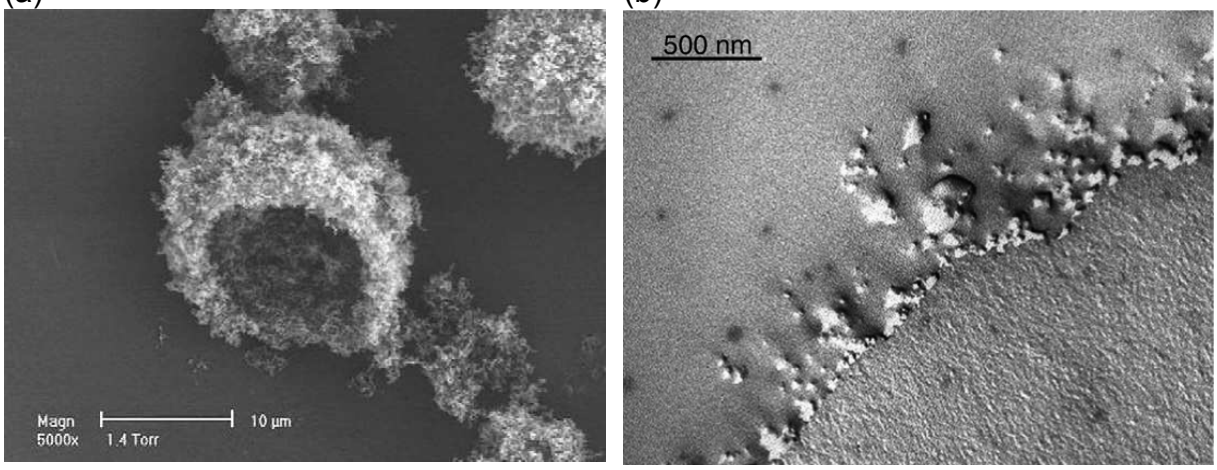

Figure 8: *(a) Broken dry water droplet (96 % water content)after water sublimation; (b) part of the silica coating of a DW particle; (L. Forny et al., 2007)*

The dry water particulates are formed by self-assembling of the silica particles around the water droplets while mixing. The strong interaction between the silica particles is attributed to the van der Waals forces, reinforced by particle entanglements (L. Forny et al., 2007). Whereas the interaction of the hydrophobic fumed silica at the water/air interface is not fully elucidated yet. It was found that there is a strong adhesion between particles and water surface, which was described as "a spontaneous phenomenon such that any particles could spontaneously attach to the interface of any liquid" (L. Forny, 2011). Figure 9 shows a water droplet brought into contact with a bed of highly hydrophobic fumed silica particles. The particles adhere to the surface of the liquid droplet.

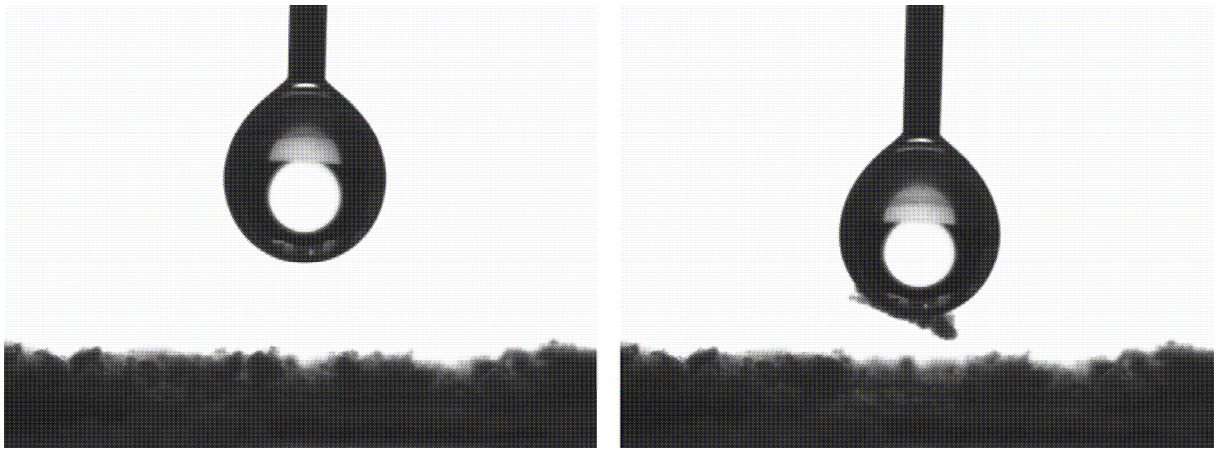

Figure 9: *Adhesion phenomenon of hydrophobic silica particles on water surface, (L. Forny, 2011)*

Investigations revealed that the surface pressure of a particle/water interface increases progressively when the surface area is decreased (L. Forny et al., 2007). Thus, an increasing stability of dry water droplets can be reached with decreasing droplet diameters.

But still the integrity of the silica shell is limited. Droplet dissociation can occur when dry water is exposed to pressure and pressure change as well as from freezing/thawing processes (B. O. Carter et al., 2010).

The dry water stability can be improved by adding gellan gum in the system. This water-soluble polysaccharide has a larger viscosity than water acting as a gelling agent. A ratio between 3 % and 10 % increases the stability of the water droplets with insignificant impairment to the dry water characteristics (B. O. Carter et al., 2010).

4.4. Required conditions

In order to obtain a proper powder formation of encapsulated water droplets, two conditions must be fulfilled. First, small water droplets must be available in the mixing process in order to get coated by silica particles. And second, the silica particles must be able to form a coating by interacting between themselves and with the surface of the water droplets.

4.4.1. Mixing conditions

In order to ensure small individual droplets in a high rotational blender, different impeller designs were investigated. The most efficient impeller for a minimum of energy input turned out to be a helical propeller causing polyvalent conditions. Strong stirring conditions initiate droplets formation while high shear characteristics perform size reduction. Furthermore the propeller produces axial and radial flow inducing a strong turbulent condition and avoiding stagnant zones in the vessel. With this device the rotational speed can be reduced down to 6000 rpm for at least 30 s, depending on the quantity. At lower mixing rates, liquid water will remain separately from the silica particles, even if the mixing time is increased. Only higher velocities up to 18000 rpm can reduce the necessary time to at least 10 s. (L. Forny et al., 2007).

In order to ensure an effective dry water preparation with atomized water at low a low mixing speed, specific conditions must be required. Atomization pressure, stirring conditions and distance between spraying nozzle and mixed material has to be precisely controlled. The atomization pressure must be higher than 8 bar and a maximum droplet diameter of 80 µm is necessary. To obtain a uniform mixing a planetary mixer with a rotating speed of 155 rpm is recommended. The impeller makes simultaneous rotation and gyration motions which reduces the stagnant zones

inside the bowl. Alternatively, for even larger quantities, a cement mixer can also be used. The spraying nozzle must be placed in a right position ensuring a maximum distance of 10 cm and an inclination angle of 45° (L. Forny, 2009; L. Forny et al., 2007).

A low shear mixing process with atomized water is much more sensitive to the operating conditions since several parameters must be fulfilled. But as a benefit the particulates produced in this system are much more spherical, especially for increasing particle diameter (Figure 7 (b), page 19). Also large quantities of dry water can be produced at a lower energy intake than high shear mixing processes require.

4.4.2. Silica particle conditions

The colloidal size, hydrophobicity and fractal shape play key roles for the encapsulation of water droplets. It is not fully elucidated yet how the powder formation precisely emerges, but especially the hydrophobicity significantly influences the occurrence of dry water. If the fumed silica is too hydrophilic, the mixing result will be a viscous liquid dispersing particles in the water. Higher hydrophobic particles lead first to a homogenous mousse resembling whipped cream which can be described as an air-in-water emulsion (Binks & Murakami, 2006). Further increasing hydrophobicity will finally enable a powder formation (Figure 10(b)).

Irregular shapes of the silica particles and therefore a high specific surface area benefit a stronger coherence between the particles due to entanglements. Stronger interactions can lead to more stable dry water droplets or a higher water content respectively.

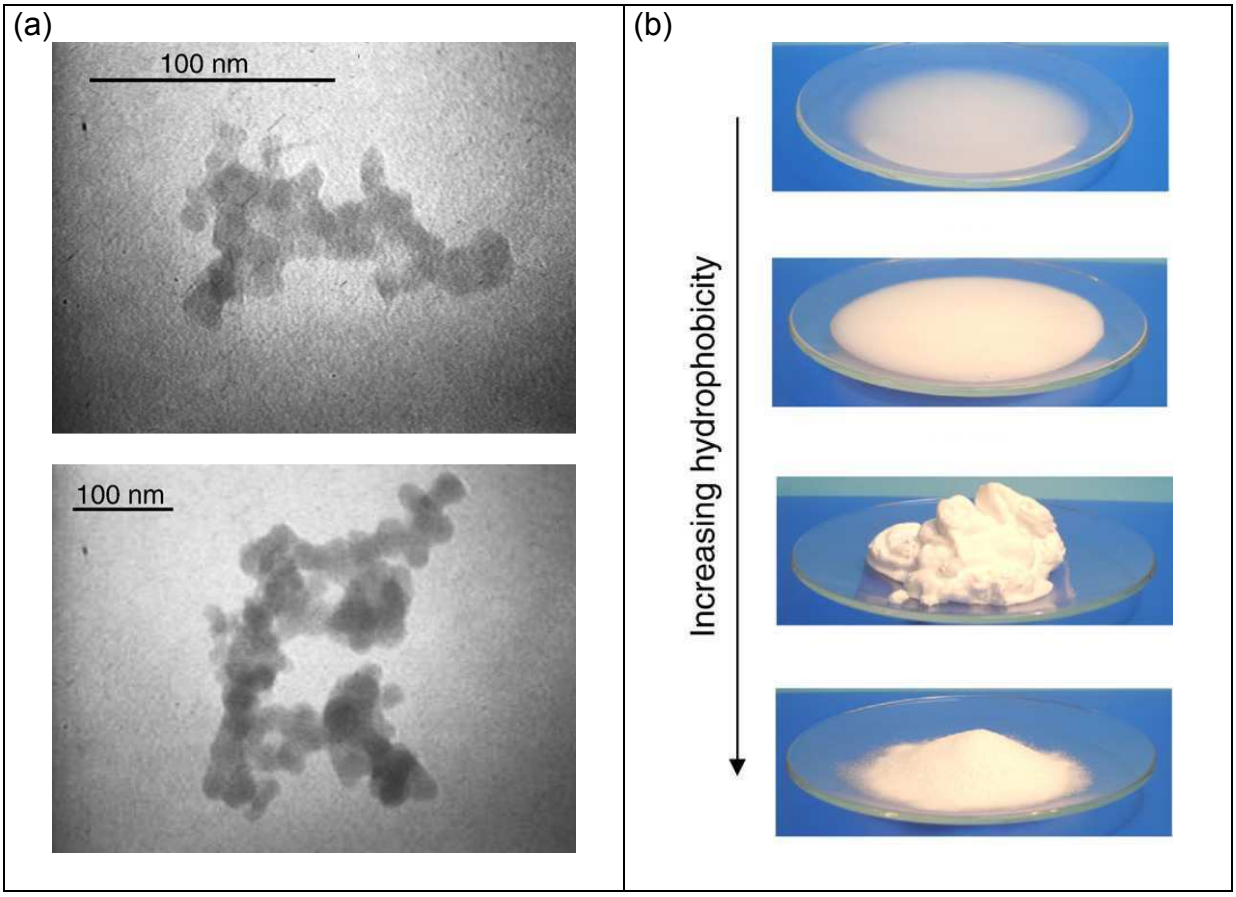

Figure 10: *(a) Fumed silica particles with increasing hydrophobicity and surface area (L. Forny et al., 2007); (b) influence of hydrophobicity on final product quality (96 % water content) (L. Forny, 2009)*

The primary fumed silica particles have a typical size of 10 - 20 nm, forming the agglomerates (Figure 10a) with a size of 0,1 - 1 µm. The residual silanol content (SiOH) representing the hydrophilicity must be less than 30 % (Binks & Murakami, 2006).

4.5. Gas uptake

Uncombined bulk water has a certain capacity of absorbing gases like methane or carbon dioxide (Berner & Berner, 1987). Attributed to the large surface of small silica coated droplets, the dry water system shows an enhanced gas uptake rate. Especially the kinetics of gas hydrate formation trapping a guest gas in the lattice of the water droplet is increased significantly.

When dry water is cooled under initial pressure (8,5 MPa) and in the presence of a guest gas like methane or carbon dioxide, the gas starts forming hydrates within few hours. One volume of an ideal exploited methane hydrate contains 180 volumes of its gas at standard temperature and pressure (Sloan, 2003). Carter et al. reached a methane uptake in dry water of 175 volumes, corresponding to 97 % of the maximum. The droplet size played a key role where the maximum uptake could be reached with the smallest droplet size (B. O. Carter et al., 2010, Wang et al., 2008).

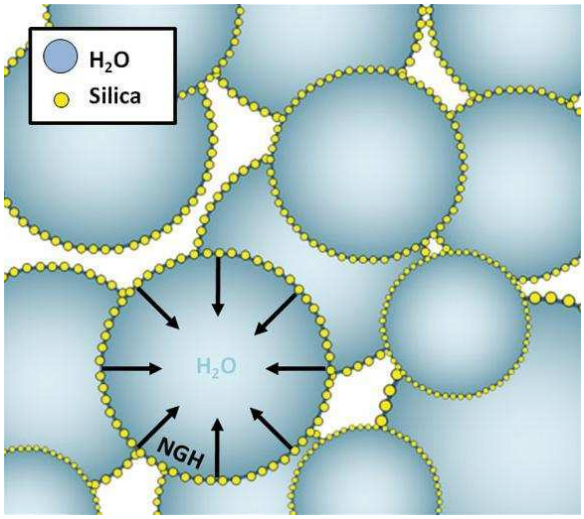

Figure 11: *Schematic of a dry water droplet containing natural gas hydrate (NGH); www.soci.org*

Compared to natural gas hydrates forming over days and months in deep seas (>500 m) or laboratory produced gas hydrates with normal water requiring high pressure and vigorous mechanical mixing, dry water gas hydrates formation shows to be more efficient. No need of stirring and an improved formation time from days to hours saves energy in the production while the dry water gas hydrates can be stored at lower pressure than usual. Dry water can absorb over three times as much carbon dioxide as ordinary, uncombined water and silica in the same space of time. Gas hydrates in dry water are stable for significant periods at atmospheric pressure with cooling (B. O. Carter et al., 2010).

This dry water with natural gas hydrates leads to a flowable powder containing a large amount of gas which can be extracted simply by warming up.

By using gellan gum (3 % - 20 % by weight) in the dry water preparation, the droplets can be stabilized in order to get more robust against dissociation while thawing ensuring a reuse for further hydrate formations (B. O. Carter et al., 2010; Wang et al., 2008).

4.6. Dry water-like powders

Not only pure water droplets can be encapsulated by silica particles. It is possible to prepare dry acids, dry alcohols and dry gels as a powdery substance. Since the same strong hydrophobic silica particles are responsible for the powder formation, the substances getting mixed with them must have a hydrophilic characteristic. But also a dispersion of fine oil droplets in water can be blended with silica particles forming a dry water emulsion without disrupting the oil droplets, a so-called oil-in-water-in-air emulsion (Binks & Murakami, 2006; B. Carter, 2010).

The highly distributed gas-liquid interface in "dry water" powders enables straightforward chemical reactions. A significantly kinetic increase of a hydrogenation of maleic acid to succinic acid could be shown by Carter and co-workers. In that case a mixture of water and maleic acid were prepared like dry water by blending it with silica particles and a catalyst (Ru/Al_2O_3), which was indistinguishable from dry water formed with pure water (Figure 12). A chemical reaction could be easily carried out by injecting the reaction gas in the system without the need of stirring (B. O. Carter, 2010).

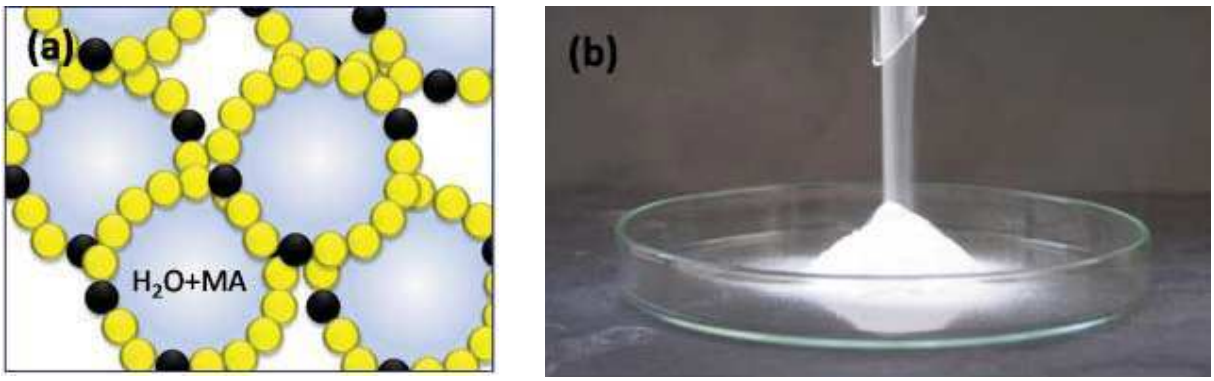

Figure 12: *a) Schematic of dry water droplets containing maleic acid (MA), surrounded by silica particles and catalyst particles (black); b) Dry water emulsion containing maleic acid; (B. O. Carter, 2010)*

5. Materials & Methods

The experimental work took place in the laboratory of LTU. All water used in this study was tab water (20°C, pH = 7,4) from the laboratory. Since the maximum quantity of each prepared dry water sample was not more than 100 g, usual laboratory glassware like 150 ml beakers were used for handling. Photographs were taken with a Kodak C613 digital camera.

5.1. Fumed silica

The fumed silica particles of the HDK® range were kindly provided by Wacker Chemie AG as a free sample of 270 gram.

Referring to the safety data sheet of Wacker, the particles are stable, no reactive, non-toxic for organisms and there are no environmental problems expected by appropriate handling (Wacker Chemie AG, 2006). But since the particles of pyrogenic silica are very small, the handling can lead to inhalable and respirable dusting. Also the product degreases the skin when getting in direct contact.

To provide a higher level of protection, the practical work took place in a common modern fume hood in the laboratory of LTU. To avoid direct contact with the skin, rubber gloves were used.

The physio-chemical properties of HDK® H2000 used in this study, presented in Table 1, are specific properties provided by the supplier.

Table 1: *Physio-chemical properties of HDK® H2000*

Primary particles size	12 - 14 nm
Sintered aggregate size	100 - 200 nm
Density at 20°C (SiO_2)	approx. 2200 g/L
BET surface	approx. 150 m²/g
Tapped density	approx. 200 g/L
Carbon content	approx. 2,8 %
Residual silanol content	25 %
Surface modification	Trimethylsiloxy

5.2. Dry water preparation

The mixings were performed with a “ES3 xpress” from Blendtec, a conventional domestic kitchen blender with lid (Figure 13). The only modification was the blunt blades providing a higher turbulent flow in the vessel. After pouring the water in and placing the particles on top, the mixing was achieved at the maximum speed of 14000 rpm for 60 seconds. It was carried out in two 30 seconds bursts to minimize heating and droplet dissociation while mixing.

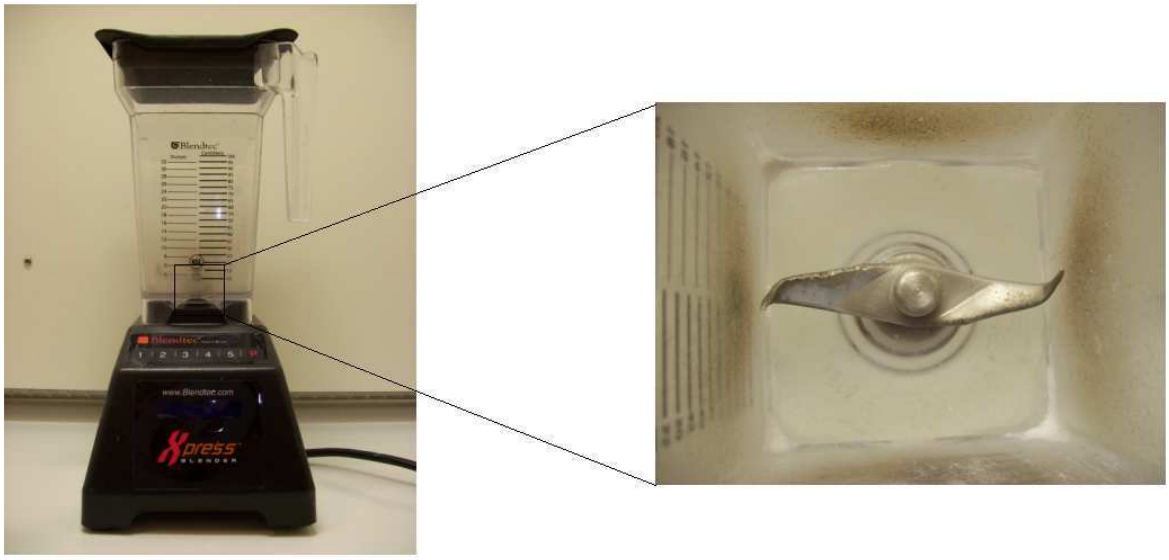

Figure 13: *Blendtec ES3 xpress with helical knife blades*

All prepared samples were transferred into glass bottles hermetically closed to avoid water loss due to evaporation before further analysis.

5.3. Microscope observations

In order to estimate the droplet sizes, an optical stereo microscope Nikon SMZ-U with an ocular scale and a camera adapter were used. With this microscope it was possible to explore a whole sample of several grams in a common Petri dish and to evaluate the mean droplet diameters.

Individual dry water droplets were observed with a Nikon Diaphot 300 microscope fitted with a NIKON E4500 digital camera. For this observation, single dry water particulates had to be separated from the sample to be very thin and transparent. Therefore a small amount of each dry water sample was put with an inoculation loop, 1 µl, into a centrifuge tube filled with 250 µl pure water. The high dilution achieved a separation of small droplets. With a micropipette, 50 µl of each preparation were applied on a diagnostic slide which could be observed under the microscope.

5.4. Powder Characterization

For initial studies on dry water, several dry water samples with different water contents were prepared. This allowed a comparison of the obtained characteristics of the products. Dry water with a specified water content which has been proved to have the most appropriate powder characteristics was chosen for more detailed studies.

Because of possible evaporation or water release under pressure, the characteristics of the powder might have changed during the tests especially under specific pressure and temperature conditions or under strong mechanical stress. For these reasons, special attention was given to ensure the powder stability during the experiments.

5.4.1. Density & Air content

In order to measure the density of the samples, a known mass of dry water was placed in a measuring cylinder to determine its volume. It was carried out using a 250 ml graduated glass cylinder. The weight was measured by a Mettler PK 300 scale with an accuracy of 1 mg.

The resultant density could be calculated with Equation (5.1):

$$\rho = \frac{m}{V} \qquad (5.1)$$

The air content could be illustrated by comparing the theoretical calculated true density without air ρ_0 with the measured value. It was calculated with densities of ρ_w = 1000 g/L for water and ρ_p = 2200 g/L for the SiO_2 - particles. The SiO_2 - specification was provided by Wacker and must be understood as the pure density of silicon dioxide of the particles without consideration of intermediate air space.

The true density of dry water ρ_0 could be calculated from the relations of its water and particle volumes (Equation (5.2) and (5.3)).

$$\frac{m_{DW0}}{\rho_0} = \frac{m_w}{\rho_w} + \frac{m_p}{\rho_p} \qquad (5.2)$$

$$\rho_0 = \frac{m_{DW0}}{\frac{m_w}{\rho_w} + \frac{m_p}{\rho_p}} \qquad (5.3)$$

Together with the measured density ρ, the air content can be determined by Equation (5.4):

$$\varphi = (1 - \frac{\rho}{\rho_0}) \cdot 100 \qquad (5.4)$$

5.4.2. Freezing properties

Since pure water shows significant properties in the volume/density change and mass loss while freezing, it was well worth to investigate it on dry water. Particularly the fact that dry water at below-zero temperatures still remains flowable, deserved a special study. This behavior was first described in 1977 in a US patent (Barry D. Allan, 1977). It may be considered an undercooling of the small water droplets without freezing. Studies have shown a lower mean freezing temperature at decreased water drop diameters where water droplets with a diameter of 100 µm could be cooled up to -30 °C K before freezing (Bigg, 1953).

Samples of dry water preparations were cooled in a freezer to -20 °C. The first step was the investigation of dry water samples with the different water ratios. The flowability in frozen state as well as the behavior after several freezing/thawing cycles were studied.

In order to investigate the ice formation or undercooling of dry water droplets respectively, the volume change and the mass loss while freezing were determined. In this tests, only dry water with a specially chosen water content were taken. To ensure an accurately measurement of volume change, a small 10 ml graduated cylinder with a division scale of 0,1 ml were used. A well known mass of dry water were filled into the measuring cylinder and the volume change at different temperatures were recorded.

In order to comprehend whether and in what extend the water droplets freeze, the mass loss over the time were investigated. Since there is a larger mass decrease while ice formation due to heat release than liquid water has due to evaporation, the rate of freezing progress can be concluded.

5.4.3. Flowability

A rotational viscometer Visco Star - L from Selecta was used to evaluate the viscosity in mPas directly at different shear rates. It is based on measurements of the torque necessary to rotate a spindle immersed in the powder at a constant angular velocity.

The test was performed with two different special spindle devices rotating in a 600 ml glass beaker. Various velocities between 0,5 rpm and 200 rpm were adjusted and the corresponding values were recorded.

With the provided equipment of the viscometer, it was not possible to measure the direct shear rate. But since the shear rate can assumed to be directly proportional to the rotational velocity (Cullen, 2003), a doubling of rotation speed causes a doubling of the shear rate. In this way the dependence of the change of shear stress on the viscosity can be demonstrated and statements regarding the flow behavior could be made.

Another quick and straightforward method is the appreciation of the flowability from the angle of repose. This measurement gives the steepest descent of the slope relative to the horizontal plane when deposited to a cone-shaped mound.

For this purpose, the powder was poured through a glass funnel onto a flat surface, obtaining a conical deposition. The funnel had a circular opening of 8 mm and a slope of 60° to the horizontal. The angle of repose for the cone was determined using geometric considerations.

This type of experiment allows an estimation of the extent of cohesiveness and thus the flowability. The lower the angle of repose of a material, the more flowable it will be. Cohesive powder have a large angle of repose (>60°), whereas the angle of free flowing powders is smaller than 25° (R. Carr, 1965).

The flow properties of powders can also be indicated by the compressibility. It is the relative volume change and can be evaluated from the tapped density and the aerated density.

The poured density of dry water immediately after filling into a graduated cylinder was assumed to be the aerated density $d_{aerated}$.

After filling the cylinder, the powder was progressively tapped for 10 minutes until a steady state has been reached (approximately 3000 tabs). Special attention was given that no water was released in the cylinder.

The tapped volume after shrinkage yielded the tapped density d_{tapped}. The compressibility C could be calculated with Equation (5.5):

$$C\ (\%) = \frac{d_{tapped} - d_{aerated}}{d_{tapped}} \cdot 100 \qquad (5.5)$$

Cohesive powders have a high compressibility (>40%), free flowing powders have a low compressibility of less than 20% (R. Carr, 1965).

5.4.4. Heat capacity

The heat capacity was assessed theoretically and experimentally, whereby the values were related to its mass, which gave the specific heat capacity in $\frac{kJ}{kgK}$. The approach of determining is based on the heat absorption $\triangle Q$, which can be calculated with the temperature change $\triangle T$ (Equation (5.6)):

$$\triangle Q = m \cdot c \cdot \triangle T \qquad (5.6)$$

where

$\triangle Q$ = thermal energy change [kJ]

m = mass [kg]

c = specific heat capacity $[\frac{kJ}{kgK}]$

$\triangle T$ = Temperature change [K]

The prevailing pressure was assumed to be the constant atmospheric pressure.

For the theoretical approach, the fumed silica particles were assumed to be pure silica dioxide. According to the manufacturer the SiO_2 - content of the particles was higher than 99,8 % (Wacker Chemie AG, 2011). Therefore the specific heat capacity of the particles was taken to be 0,725 $\frac{kJ}{kgK}$ which is the value of amorphous SiO_2 - particles at 295 K (Andersson, 1992). The value for water at 22 °C is c_W = 4,184 $\frac{kJ}{kgK}$ (VDI heat atlas). The small mass of air was considered to be negligible and thus not taken into account.

The measurement has been carried out using an insulated thermos flask. A well known mass of warm water (T_{Wo}; around 40 °C) were poured in and the temperature were measured by a resistance thermometer with an accuracy of 0,1 °C. A certain amount of dry water packed in a thin plastic bag and with a known temperature (T_{DWo}; commonly room temperature) was immersed. It was waited till the temperature decline stopped and the value were noted (T_1).

The temperature change from the water $\triangle T_W$ and the dry water $\triangle T_{DW}$ is given by the following Equation (5.7) and Equation (5.8):

$$\triangle T_W = |T_{Wo} - T_1| \qquad (5.7)$$

$$\triangle T_{DW} = |T_{DWo} - T_1| \qquad (5.8)$$

For the consecutive calculations the mass of the plastic bag (index PB) were considered. The bag consisted of polyethylene with low density (PE-LD) which has a specific heat capacity of $c_{PE\text{-}LD}$ = 2,4 $\frac{kJ}{kgK}$ (Carlowitz, 1986). It was sealed with a knot and the rest of the plastic were cut off to minimize the mass of foreign material. Each mass were measured accurately and the values were taken into account. It was calculated as follows:

$$Q_W = Q_{DW} + Q_{PB} \quad (5.9)$$

$$m_W \cdot c_W \cdot \triangle T_W = m_{DW} \cdot c_{DW} \cdot \triangle T_{DW} + m_{PB} \cdot c_{PB} \cdot \triangle T_{PB} \quad (5.10)$$

The temperature change of the dry water and the plastic bag was the same $\triangle T_{DW} = \triangle T_{PB}$. Taking Equation (5.10), the specific heat capacity for dry water could be calculated:

$$c_{DW} = \frac{m_W \cdot c_W \cdot \triangle T_W - m_{PB} \cdot c_{PB} \cdot \triangle T_{DW}}{m_{DW} \cdot \triangle T_{DW}} \quad (5.11)$$

A factor of uncertainty influencing the measurements negative was the lid of the thermos flask. It was not insulated perfect and heat could dissipate. This heat loss became noticeable in a very slowly but constant temperature decrease. Before the experiment had been started, the temperature decrease of 40 °C warm water (approx. 120 gram) in the insulated flask were measured over the time. It showed a gradient of 0,1 Kelvin per minute, which was considered in the computations.

After immersing the dry water sample into the bulk water, special attention were taken to the rapidity of temperature change. As soon as the fast temperature change stopped (commonly after 60 seconds) the value were noticed.

6. Results and Discussion

6.1. Dry water preparations

For the first test of preparation, the fumed silica particles were poured into a water filled glass beaker while stirring by hand with a small whisk.

But mixing by hand soon proved to be unusable, since the energy input was not enough to get fine water droplets which can be surrounded by silica. As a result both products kept separated with the particles floating on the water (Figure 14) due to the strong hydrophobicity of the silica particles.

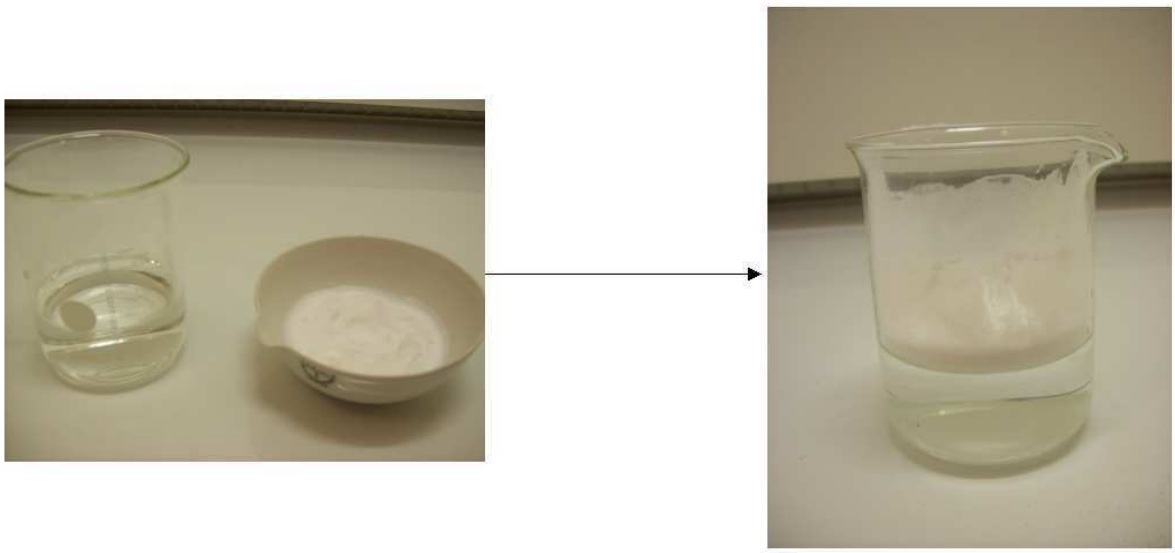

Figure 14: *95 g water and 5 g silica particles; after stirring with a whisk*

6.1.1. Dry water with 95 wt% water

For the first sample, a ratio of 5 g silica particles and 95 g water were mixed with the blender in two 30 s bursts. The result was a free-flowing “dry” powder looking like powdered sugar. It could easily be poured from one vessel into another without any residues of free water. By turning the vessel, the substance moved like a viscous liquid, resembling dough. But when poured into another vessel, it flowed and behaved visually more like a powder.

Figure 15: *Dry water with 95% water by weight*

6.1.2. Dry water with 97 wt% water

97 g water with 3 g silica particles could likewise be mixed successfully. Against expectations, that the mixture could contain free water, a homogeneous blend was formed where virtually all the water was taken up as stable drops. But in contrast to the sample with 95 wt % water content, the droplets were much larger in size and they were merged to a mousse resembling whipped cream (Figure 16(a)). Tactile examination revealed a release of water since in felt far more wet when getting in contact with the skin.

Its foamy appearance also showed appropriate properties. After pouring into a funnel, it remained there without draining (Figure 16(b)). Only after lightly mechanical tapping on the funnel the substance could partial flow off. It could not be described as a free flowing powder anymore.

(a) (b)

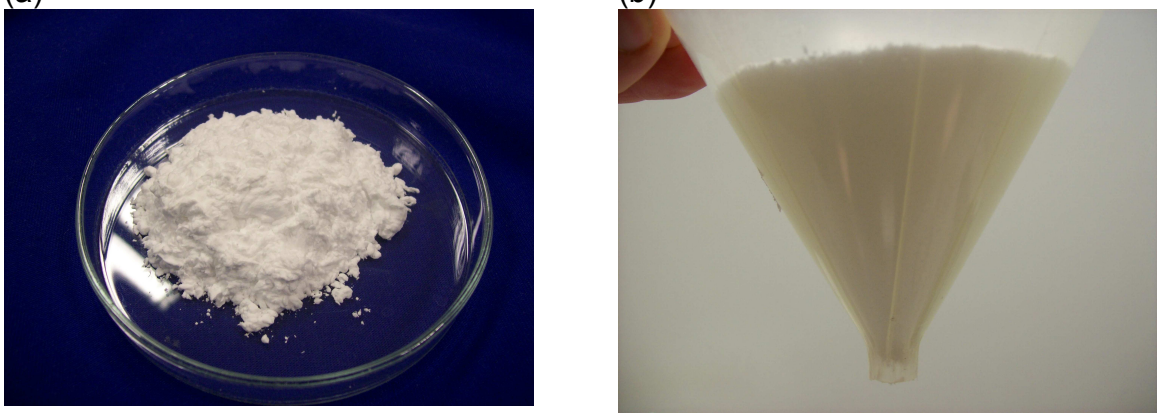

Figure 16: *(a) Dry water with 97 % water content resembling whipped cream; (b) in a funnel without flowing off*

6.1.3. Dry water with 90 wt% water

The result of blending 90 g water and 10 g particles was a very fine powdered substance where each powder particle was visually much smaller (Figure 17). It behaved more like a powder when poured through a funnel without leaving any residues. Also no residuals on the skin could be recognized when it got in contact and it felt drier compared to the other dry water samples.

Figure 17: *Dry water with 90 weight% water content poured through a funnel*

All three dry water preparations with the blender were made in the same way under same conditions. Each mixing burst of 30 seconds led to a temperature increase of 2 °C due to friction while blending, but it had no provable impact on the final result. At each prepared sample a total water absorption of the silica particles were achieved with no trace of liquid water. The formation were stable enough against water release while pouring it or shaking the closed vessel. But nevertheless water could be easily released each time by rubbing it onto the skin.

Decreasing the water content to less than 90 % by weight brought no more benefits in powder formation regarding smaller droplet size and visual flowability. Only an incipient part of free silica particles could be observed.

The initial test of stirring water and silica particles by hand showed that a higher energy input in form of high rotational speed is required. This provides a domestic blender.

Differences could be made between each preparation from visual and tactile examinations. The samples with larger water content had a more powdery trait with a finer droplet size distribution. The good flowability of the dry water with 90 % water content suggest more individual and stable droplets with less coherence between them. The sample containing 97 wt% water (Figure 18(a)) cannot be described as a common powder anymore. In that case, particles could interact in a network involving air to form a mousse instead of dry water.

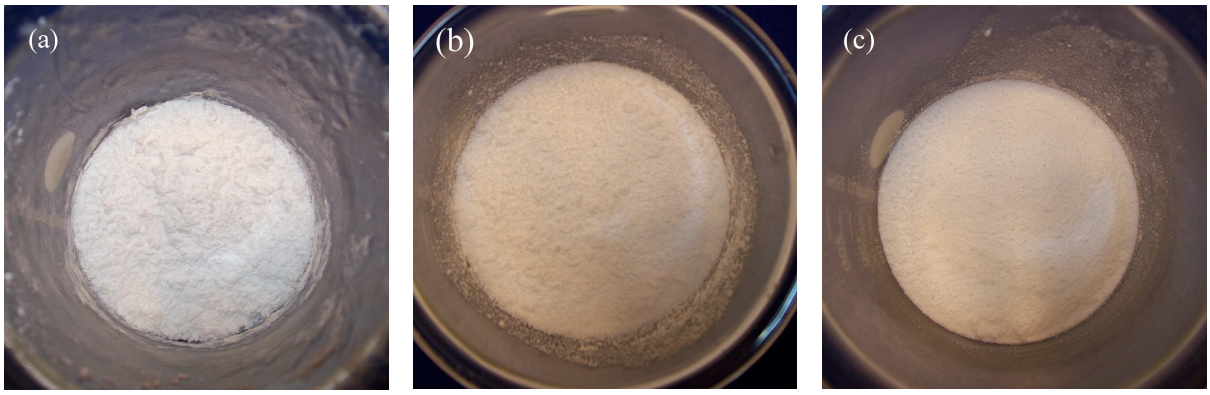

Figure 18: *Dry water containing (a) 97 % water, (b) 95 % water and (c) 90 % water by weight*

6.2. Droplet size

The stereo microscope revealed a wide range of droplet sizes and the droplets occurred in various shapes with irregular outlines. It could be observed a strong accumulation of very small particulates to larger droplets. Even some larger droplets were not recognizable as an accumulation of small particles (Figure 19(c)). The smallest droplets were approximately spherical whereas larger ones appeared rather elongated. The mean size of larger droplets could be constituted between 50 µm and 200 µm in the dry water with 90 wt% water content and about 200 µm to 400 µm at the sample with 95 wt% water. In the foamy preparation sample was a visible coalescence of the silica coated droplets. The powder particulates were not distinguishable enough from each other anymore in order to make good predicate about their size (Figure 19(a)).

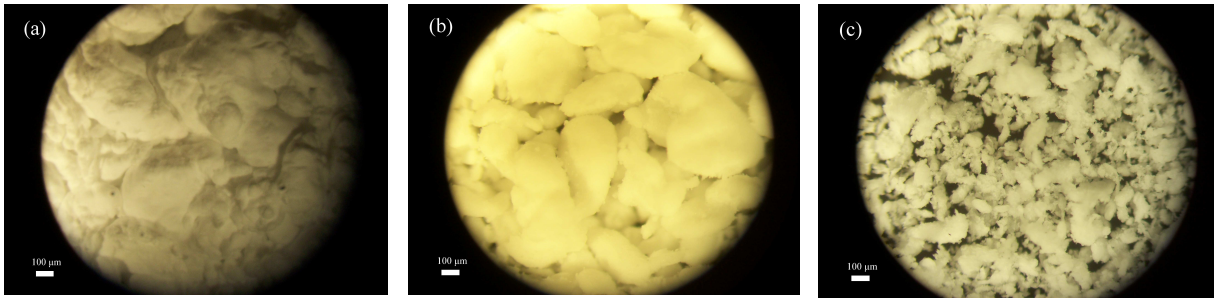

Figure 19: *Microscope images (50x magnification) showing dry water containing (a) 97%, (b) 95% and (c) 90% water by weight*

The small particulates could be separated by diluting in pure water without destroying their armoured layer. With a higher resolution, their mean size could be estimated to 75 µm – 100 µm for the largest droplets, 30 µm – 40 µm for the medium size and about 10 µm for the finest dry water powder (Figure 20).

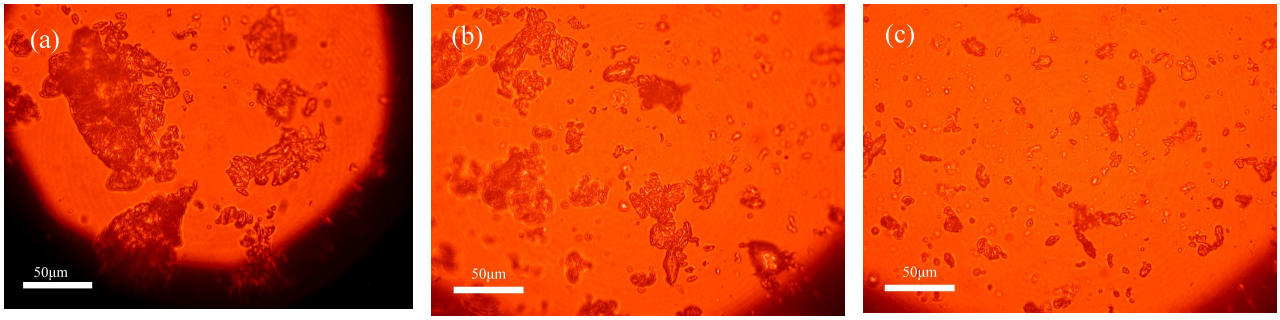

Figure 20: *Microscope images (200x magnification) showing dry water droplets from dry water with (a) 97wt%, (b) 95wt% and (c) 90wt% water content*

Although the estimation under the microscope was not the most accurate method to measure to exactly sizes, it gave a good appraisal of the size range in which the particles varying at different preparations.

Since the mixing speed and thus the energy intake was the same in all three preparations, the bulk water phases were dispersed to individual droplets with the same size in all dry water samples. In relative terms, less supplied silica particles lead to a partial re-coalescence of the water droplets to larger sizes till the hole particles are enough to provide a stable network. At less water contents more silica particles are available to wrap a larger water surface and therefore all dispersed water droplets. Although the silica network still exists when the water content is larger than 95 % by weight, it does not cover individual water droplets anymore giving a foamy appearance.

In general it could be said that a lower water content leads to smaller droplet size.

6.3. Density

After pouring the dry water into the cylinder, an instant slow-going decrease of the volume over up to 120 seconds were observed. The volume was noted in both cases, directly after filling and after the decrease.

The extent of volume shrinkage was not always the same, it greatly depended on the ratio of particles and water, respectively the droplet size. The largest decrease of volume were observed at the preparation with the smallest droplet size whereas the shrinkage at the dry water with 97 wt% water content stopped already after

20 seconds. Figure 21 shows the density in dependence of the dry water preparation after filling and after the volume decrease.

The poured density and the bulk density were found to be respectively 372 g/L and 570 g/L for the powder with 90 wt% water content and 664 g/L and 708 g/L for 95 wt% dry water. For the dry water with 97 wt% water content these values are 732 g/L and 757 g/L (see also Appendix I: Density).

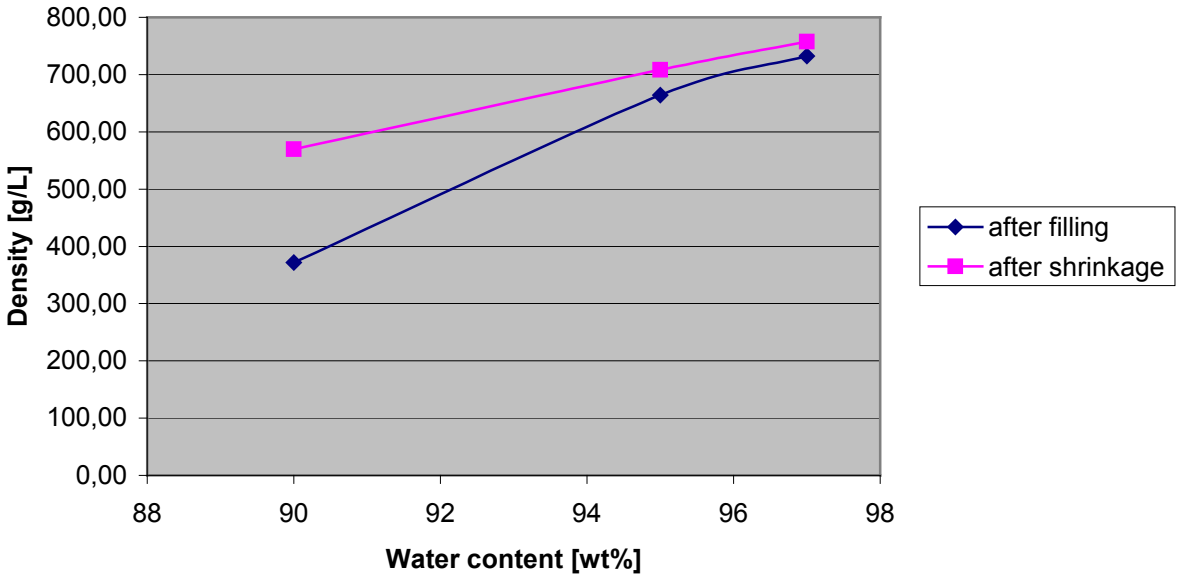

Figure 21: *Densities of different dry water preparations*

In general, the lower the water content of the dry water is, the lower is the density. More water droplets with smaller diameter were formed occupying a higher volume due to more spaces between them. This indicates the significantly higher volume reduction of the powder with 90 wt% water content. The air between the droplets removes due to the weight of the particles bearing down on them. A further reason for a volume reduction - albeit only a small one - might be the deformation of the lower droplets and therefore tighter packed layer because of the weight of the upper particles.

This significant shrinkage of the volume of course depends also on the hydrostatic pressure. Each volume change would be varying if the measuring cylinder would have had different dimensions. Unlike the measuring cylinder with a small diameter and a high column, the same amount of dry water in a large bowl will remain at a

larger volume. But it is comparable with the bulk density and tapped density and shows that the reduction is higher the smaller the particles are. The total compressibility of dry water will be determined later on (see chapter 6.6 Flowability).

6.3.1. Air content

Assuming a water content of 95 % by weight and taking Equation (5.3) (page 30), the density of dry water without air can be calculated to:

$$\rho_0 = \frac{1}{\frac{0,95}{\rho_w} + \frac{0,05}{\rho_p}} = 1028,04 \text{ g/L} \qquad (6.1)$$

The measured densities were 664 g/L directly after filling and 708 g/L after shrinkage.

With Equation (5.4) (page 30), the air content φ in dry water with 95 wt% water content is $\varphi_1 = 35,4$ vol% after filling and $\varphi_2 = 31,1$ vol% after volume reduction (shrinkage).

Figure 22 illustrates the air content at different dry water preparations, calculated with Equation (5.4). The values for 97 wt% water content are $\varphi_1 = 28,0$ vol% and $\varphi_2 = 25,5$ vol%, for 90 wt% dry water $\varphi_1 = 64,8$ vol% and $\varphi_2 = 46,1$ vol% respectively (see also Appendix I: Density)

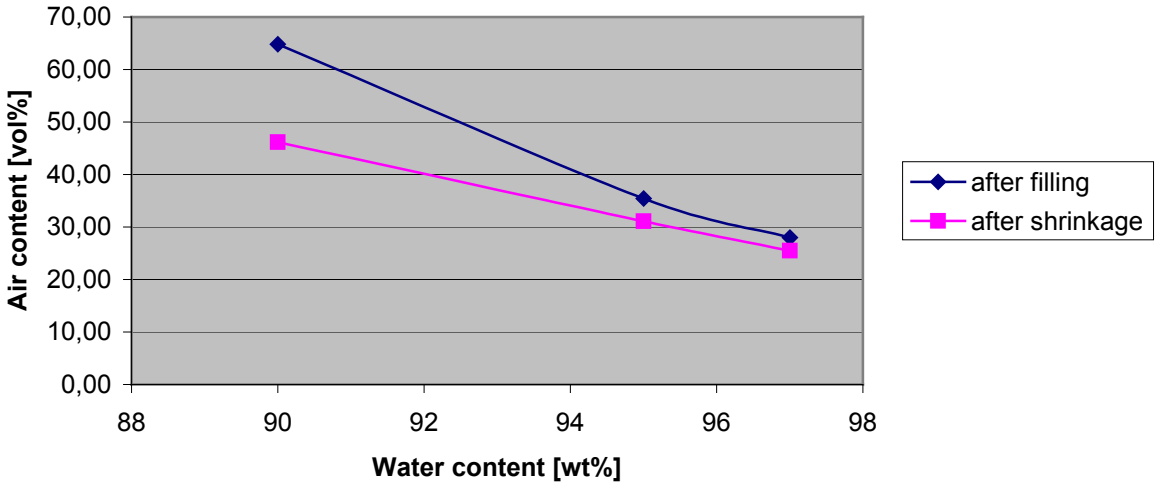

Figure 22: *Air content at different dry water preparations*

The air content after filling and after shrinkage can be understood as the air content in the aerated and tamped state. The less the water content in the dry water and therefore the smaller the mean droplet diameter the more air is enclosed inbetween the dry water particles.

It shows an increasing air content at increasing water content or decreasing droplet size respectively which is the significant reason for the density differences at various dry water samples.

6.4. Freezing properties

6.4.1. Flowability and stability at below-zero temperatures

After the three different dry water samples with 90 %, 95 % and 97 % water content by weight respectively were frozen to -20 °C, there were no visually differences, since it still looked like the same white substance like before. But when poured into another vessel, the 90 wt% dry water was still a powder and therefore pourable, while the dry water with 95 wt% water content and higher remained as a solidified piece. Though, the preparation with 90 wt% water also had a rigid crust on the

surface, but it could easily be destroyed by slightly pushes with a spoon. After destroying the solid layer, it was a powder with occasional nuggets.

Although all coated water droplets were supposed to be frozen in all three samples, only the finest powder size kept their flowability. Apparently, larger droplets coalesce among each other and cannot keep the droplets separated. Seen under the microscope, the dry water with larger droplet sizes contains some free water droplets which are not coated by silica particles anymore. Figure 23 shows dry water with 95 % water content by weight directly taken from the freezer to the microscope, some droplets started reliquefying again.

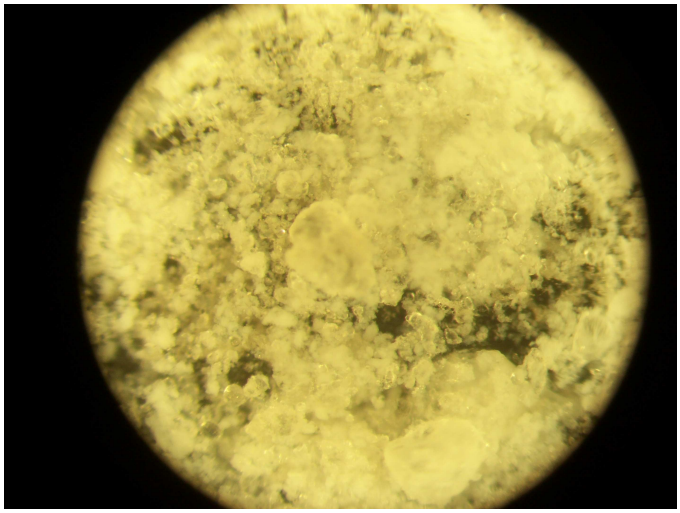

Figure 23: *Dry water after freezing (95 wt% water content)*

The reason for the solidification of the dry water powder must be the release of water from its wrapping with silica. The coatings break and free water leads to tying it all together.

The destruction of the silica coat may be seen as a freeze fracture of the droplets. When the volume of the water droplets increases while freezing, there are not enough particles available for a continuing coating due to the lower ratio of silica particles corresponding to a water unit. Also a larger droplet size leads to a higher increase in volume relatively, where more particles are necessary than existing.

After thawing the dry water with 97 wt% water content completely, a not inconsiderable amount of free water puddle could be observed on the bottom of the Petri dish (Figure 24) with the remained dry water powder floating on top.

Figure 24: *Water release after thawing (97 wt% water content)*

The smaller the droplet size of the dry water, the less water was dissociated after thawing. At the dry water with 90 % water in weight and therefore the smallest droplet size, the first separation of water were noticed only after the third cycle of freezing/thawing. The same extent of segregation like in Figure 24 was approached until after six cycles.

6.4.2. Volume change due to freezing

6 ml of dry water with 90 wt% water content, which had a mass of 2,916 g were filled into the measuring cylinder and the volume change at different temperatures were recorded. Starting with room temperature of 20 °C, it was cooled to 5 °C in a refrigerator for two hours to ensure an even temperature distribution. After cooling, the sample was put into the freezer at -20 °C for another two hours. It could be observed a total volume decrease of 0,2 ml as shown in Figure 25.

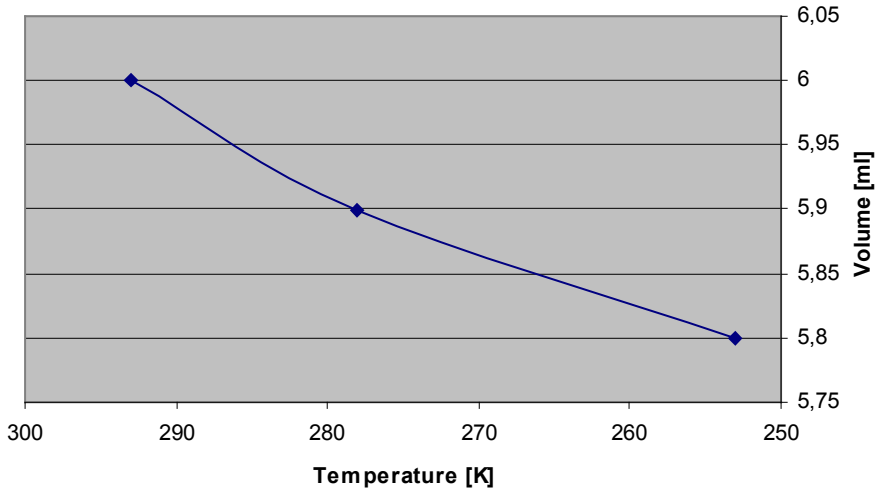

Figure 25: *Volume decrease of 2,916 g dry water while cooling*

This was against the expectations since the volume of ice expands. It might have been assumed that the coated water droplets were not frozen and thus stayed in a liquid but supercooled state. But after visual and tactile examinations, the droplets were obviously not in a liquid state since solid powder particles could be observed.

The explanation must be the relatively high air content, entailing a higher volume decrease than the expansion of the water. The following recalculation of volume change supports this assumption.

6 cm³ (ml) dry water has a mass of m_{DW} = 2,916 g and a ratio of water/silica particles of 90/10. Considering the water content, the masses for water m_W and silica particles m_P can be calculated with the following Equation (6.2) and (6.3):

$$m_W = 0{,}9 \cdot m_{DW} \qquad (6.2)$$

$$m_P = 0{,}1 \cdot m_{DW} \qquad (6.3)$$

From Equation (6.2) and Equation (6.3), the masses are m_W = 2,6244 g and m_P = 0,2916 g.

The densities of water and ice are taken as $\rho_{Water}(20\ °C) = 998{,}21$ g/L and $\rho_{Ice}(-20\ °C) = 920{,}60$ g/L (Kate White, 2005; *VDI heat atlas*). The volumes can be calculated with Equation (5.1) (page 30) to:

$$V_{Water}(20\ °C) = \quad 2{,}6291\ cm^3$$

$$V_{Ice}(-20\ °C) = \quad 2{,}8508\ cm^3$$

The difference of both volumes yields the volume change of water while ice formation:

$$\triangle \mathbf{V} = \mathbf{0{,}2217\ cm^3} \quad \text{(increase)}$$

To calculate the volume occupying the air, the volume of silica particles has to be considered. The pure density of the fumed silica particles without air content is $\rho = 2200$ g/L. (see Table 1, page 28)) . The volume occupying the silica particles calculated with Equation (5.1) (page 30) is:

$$V_P = \quad 0{,}1326\ cm^3$$

After subtracting the water and particle volume from the initial volume, the air volume is

$$V_{air} = 6\ cm^3 - V_{Water}(20\ °C) - V_P = \quad 3{,}2383\ cm^3 \qquad (6.4)$$

Considering the air density at 20 °C of ρ_{air}(20 °C) = 1,1885 g/L, (*VDI heat atlas*) the mass of air can be calculated:

$$m_{air} = \rho_{air} \cdot V_{air} = 3{,}8487 \text{ mg} \qquad (6.5)$$

From the density of ρ_{air}(-20 °C) = 1,3771 g/L, (*VDI heat atlas*) the volume of air at -20 °C is

$$V_{air}(-20\ °C) = 2{,}7948 \text{ cm}^3$$

Thus, the volume change of air from +20 °C to -20 °C is

$$\triangle V = \mathbf{-0{,}4435\ cm^3} \quad \text{(decrease)}$$

The sum of all individual volume changes arises the total volume change of the dry water sample:

$$\triangle V_{total} = -0{,}2218 \text{ cm}^2 \quad \text{(decrease)}$$

Within the framework of reading accuracy, the result corresponds to the extent of shrinkage which has been observed.

The calculation of the air volume were simplified assuming the density of dry air under normal pressure (p = 1,01325 bar). Yet, because only the differences between two different volumes were calculated, the deviation remains limited. Also the thermal shrinking of the silica particles were not considered since it is extremely low.

6.4.3. Mass loss due to freezing

The mass loss of dry water with 90 wt% water content due to freezing were compared with the mass loss due to evaporation on a similar cooled sample of 5 °C. The same experiment has been carried out with normal water in order to get a comparison.

The certain volume (app. 30 ml) of dry water and water respectively were each filled in 2 similar glass beakers with a diameter of 65 mm and thus a free surface of 33,2 cm². One sample was put into the freezer with a temperature of –20 °C, while the other sample was kept in the refrigerator at 5 °C. The initial temperature was 5 °C each time. The initial mass as well as the mass after certain intervals were recorded as shown in Figure 26 and Figure 27.

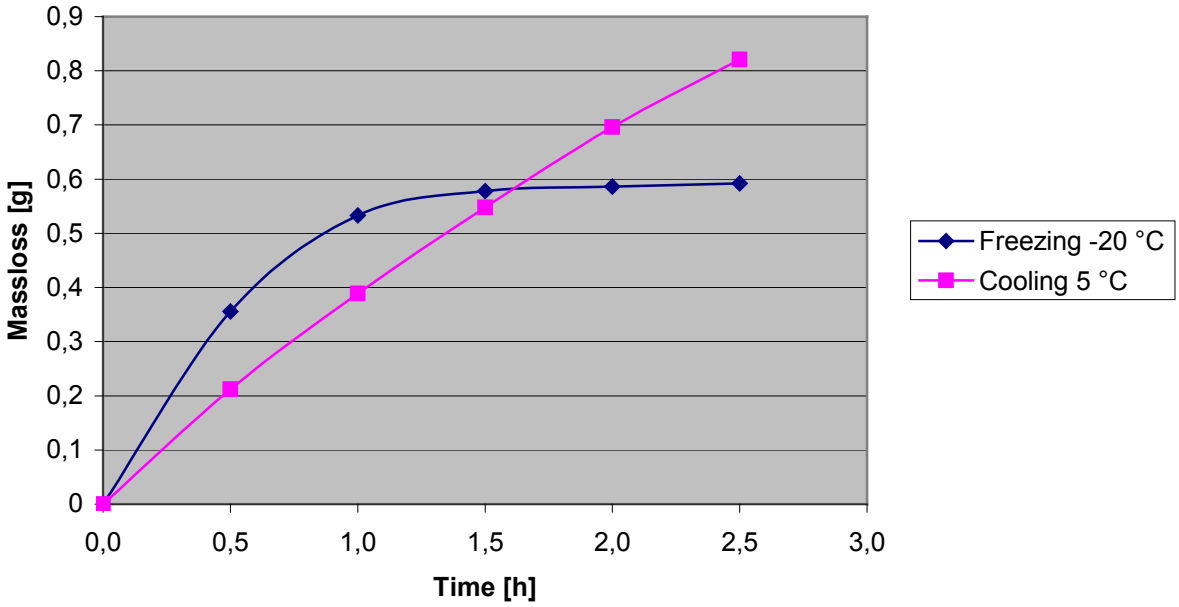

Figure 26: *Mass loss measurements for 27 g water*

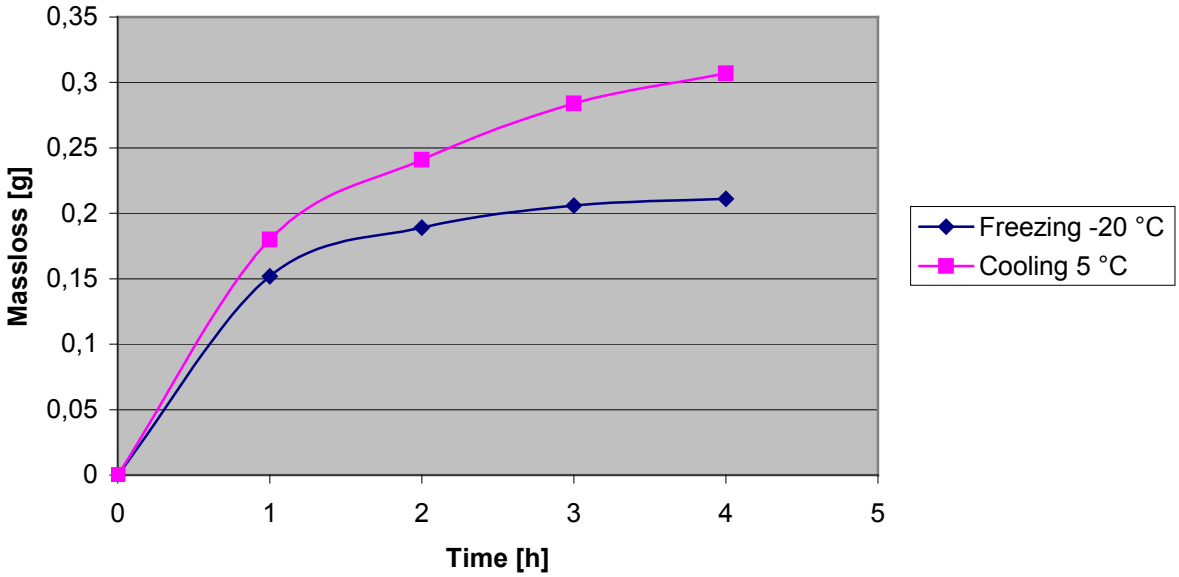

Figure 27: *Mass loss measurements for 20 g dry water (90 wt% water content)*

Bulk water (Figure 26) shows a higher rate of mass loss while ice formation than the liquid water has. After around 90 minutes the formation of ice had almost been completed and the rate of mass loss reduced significantly whereas the evaporation of water remained in the same rate. Quite significant is a larger reduce of mass at the beginning of the freezing process. The total mass loss of the frozen sample approached 0,6 g complying approx. 2,2 % of the initial mass of 27 g.

As dry water is exposed to minus temperatures, the mass loss due to freezing is less than the mass loss due to evaporation of the cooled sample at 5 °C (Figure 27). Also the relative mass loss referring to the ice mass was less than 1,1 %.

The initial mass of dry water was less than the mass of bulk water used in the experiment. Nevertheless the time period of mass decrease of dry water was about 2 hours longer than at the freezing process of bulk water. It is an indication that some dry water droplets start freezing at lower minus temperatures due to their small size. Tactile observations of dry water after 1 hour of freezing still showed apparently liquid droplets in the powder. Thus, it took a longer time for ice formation and the mass loss due to evaporation continued for a longer duration.

Since the droplet sizes have a large distribution from 10 µm to 200 µm, it is difficult to predict a freezing point. But from the observations it can be derived a shift of the freezing point to a lower temperature.

6.5. Evaporation rate

Dry Water could be stored without loss of water by evaporation in sealed vessels. But in contrast it was observed that water thoroughly evaporates in open air stored conditions, despite the protection of the water droplets by an armoured silica layer. Microscopic observations through the optical microscope revealed a visual evaporation by moving to transparent particulates (Figure 28).

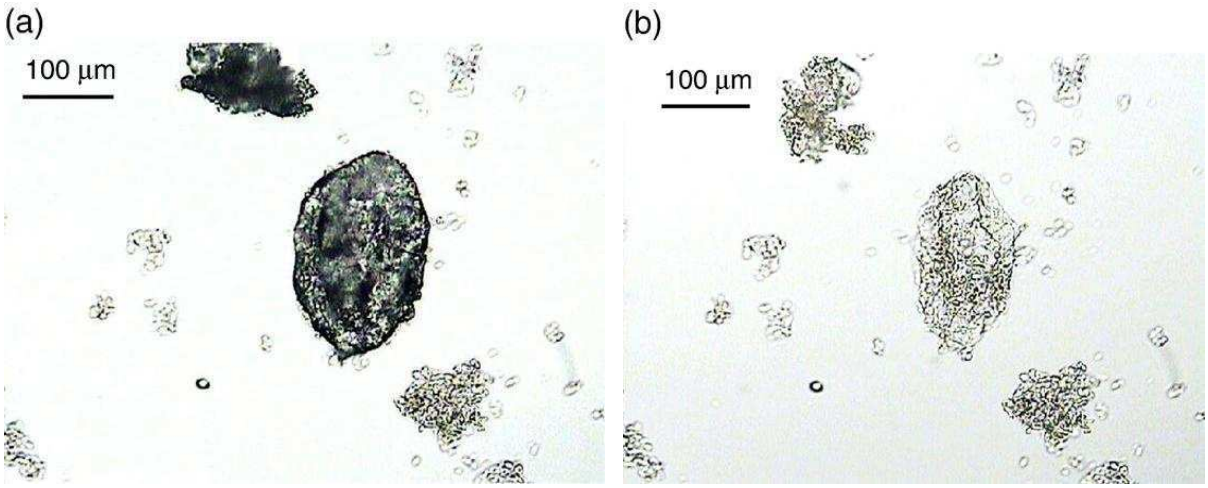

Figure 28: *A water-rich powder particle (a) before and (b) after water evaporation, (L. Forny et al., 2007)*

Figure 29 shows the result of a simple experiment, comparing four similar glass beakers with a diameter of 6,5 cm, filled with 90 wt%, 95 wt%, 97 wt% dry water and pure water respectively and leaving them for one week at room temperature. All samples were stored at the same place under same conditions.

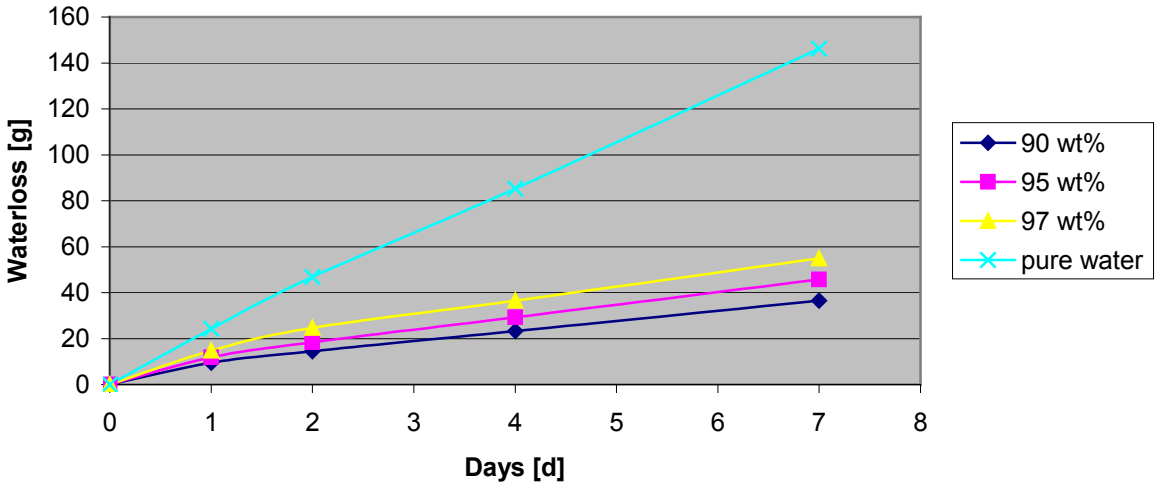

Figure 29: *Waterloss due to evaporation*

The water loss in dry water was approximately a third of the amount of water evaporated in pure water. It is interesting to note that the smallest droplet size, and therefore the dry water with the largest free surface, has the lowest evaporation of water. This suggests a stronger protection of the silica coating, which also could be observed at the thawing behavior.

Furthermore, dry water shows a slightly decreasing gradient of the curve indicating a slowdown of evaporation over the days. It can be assumed that the water evaporates in the upper part while the remained particles protect the lower water droplets from evaporation.

6.6. Flowability

The flowability depends on the internal friction of the powder caused by the adhesive and cohesive forces between individual particles. This forces are affected not only by the dry water parameters itself like droplet size and particle shape but also by external factors like shear rate and consolidation due to external forces (Schulze & SpringerLink, 2008).

As has been observed before, dry water can be more or less dilated or compressed. This leads to a large variability of interparticle contact density resulting in widely different bulk flow properties.

Thus, it is not possible to describe the flowability of dry water with only one numerical value. In order to make meaningful conclusions about the rheology of dry water nevertheless, the flow properties has been assessed by different methods.

For the determinations of the flowability, dry water with 90 % water content by weight were used since in showed the most appropriate powder characteristics.

6.6.1. Viscosity

The measurement with the viscometer showed a strongly dependence of the viscosity on the velocity of the spindle and shear rate respectively. There is a great viscosity of dry water surrounding the low-speed cylinder while the value decreases rapidly at higher velocities. The values varying from over 15000 mPas at 5 rpm to around 200 mPas at the highest rotational speed, shown in Figure 30 and Appendix II: Viscosity.

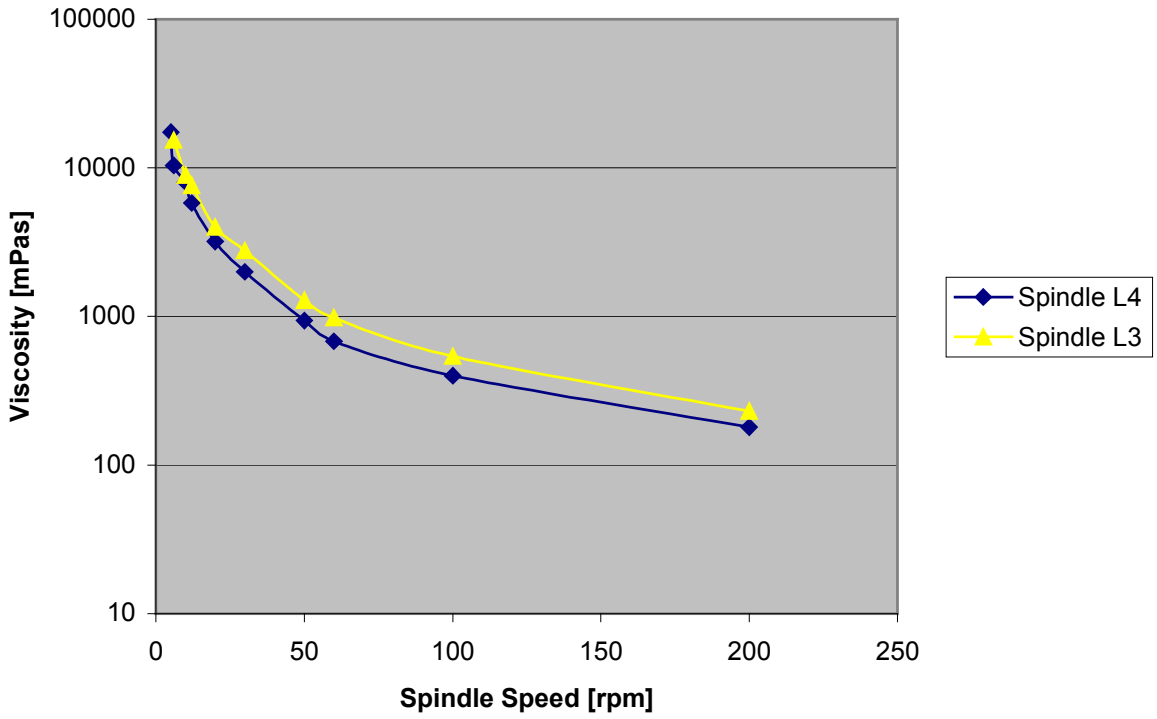

Figure 30: *Viscosity vs. spindle speed in a rotational viscometer*

This shear dependent viscosity is a characteristic behavior of powdery materials and is generally described as a non-Newtonian fluid (H. Kuno, 1967). A certain amount of force must be applied to the powder before any flow is induced attributing to the existence of static frictional resistance between the dry water droplets. Once, the static resistance is overcome the flow rating improves significantly. The value of around 200 mPas at a spindle speed of 200 rpm is comparable with the viscosity of oil.

6.6.2. Angle of repose

The angle of repose for the cone was assumed to be an average of two angles α_1 at left and α_2 at right (Equation (6.6)).

$$\alpha = \frac{1}{2} * (\alpha_1 + \alpha_2) \qquad (6.6)$$

The reason for this averaging process is that the peak point was not immediately above the center (Figure 31).

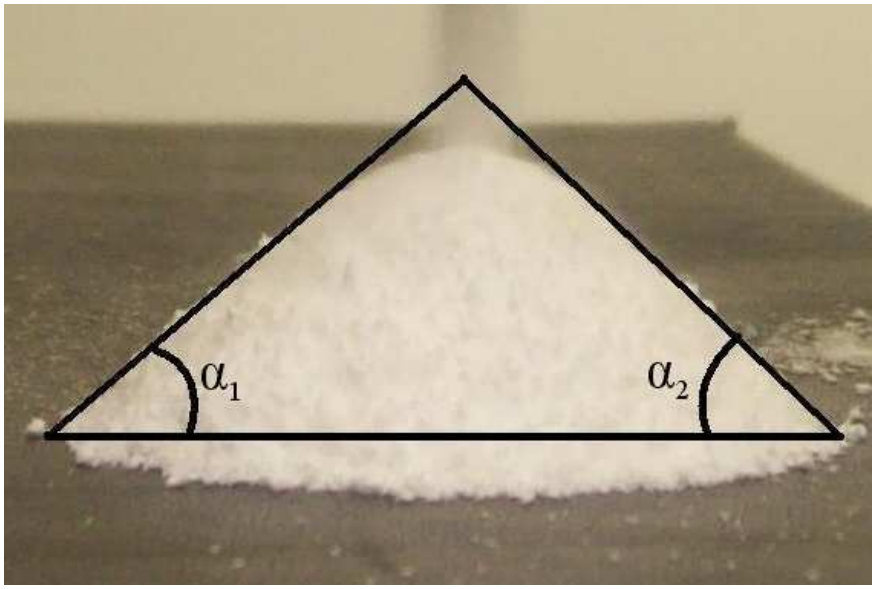

Figure 31: *Angle of repose for dry water*

The angles of the pile were found to be $\alpha_1 = 41°$ and $\alpha_2 = 44°$. Equation (6.6) then yields an angle of repose of $\alpha = 42{,}5°$.

Regarding other substances like dry sand with a good flowability ($\alpha \approx 25°$) or calcium carbonate powder with poor flow properties ($\alpha > 60°$), the repose angle of dry water reveals an intermediate level.

6.6.3. Compressibility

40,05 g dry water was poured in a 100 ml measuring cylinder which occupied a volume of 100 ml directly after filling. After about 3000 slightly taps, the volume came to a level of 64 ml. Thus, the aerated and tapped density were $d_{aerated} = 400{,}5$ g/L and $d_{tapped} = 625{,}8$ g/L respectively.

From Equation (5.5) (page 33) the compressibility could be calculated to C = 36,0 %.

The ascertained result showing here is the ability of volume reduction without increasing the pressure. According to the Carr´s classification (7 graduations going

from excellent to very, very poor flow), the compressibility can be described as passable (R. Carr, 1965).

6.7. Heat capacity

Since the dry water consists of 90 % bulk water in weight, its heat capacity can be expected to be nearly as high. Only the value for silica particles, which is relatively low compared to water, will entail a decrease. The presence of air in the dry water powder might also be an influencing factor, albeit a very small one since the mass of air is very little.

6.7.1. Calculated specific heat capacity

The theoretical value for the specific heat capacity of dry water (index DW) could be calculated from its energy uptake which is equal to the sum of its components, water and particles (index W and SiO_2, Equation (6.7)). The small mass of air was considered to be negligible and no taken unto account.

$$\triangle Q_{DW} = \triangle Q_{W} + \triangle Q_{SiO2} \qquad (6.7)$$

With Equation (5.6) (page 33), it can be written to

$$c_{DW} \cdot m_{DW} \cdot \triangle T_{DW} = c_{W} \cdot m_{W} \cdot \triangle T_{W} + c_{SiO2} \cdot m_{SiO2} \cdot \triangle T_{SiO2} \qquad (6.8)$$

Since each temperature changes $\triangle T_{DW}$, $\triangle T_{W}$ and $\triangle T_{SiO2}$, are similar, they cancel out each other. Equation (6.8) can be transformed to the theoretical specific heat capacity for dry water c_{DW} to

$$c_{DW} = \frac{c_W \cdot m_W + c_{SiO2} \cdot m_{SiO2}}{m_{DW}} \qquad (6.9)$$

Considering the relations of each mass between them at a water content of 90 % by weight ($m_W = 0{,}9 \cdot m_{DW}$ and $m_{SiO2} = 0{,}1 \cdot m_{DW}$), the specific heat capacity can be calculated as follows:

$$c_{DW} = c_W \cdot 0{,}9 + c_{SiO2} \cdot 0{,}1 = 3{,}834 \frac{kJ}{kgK}$$

6.7.2. Measured specific heat capacity

In order to increase the measuring accuracy several sessions were carried out. The single values determined with Equation (5.11) (page 35) as well as the average value are shown in the following figure.

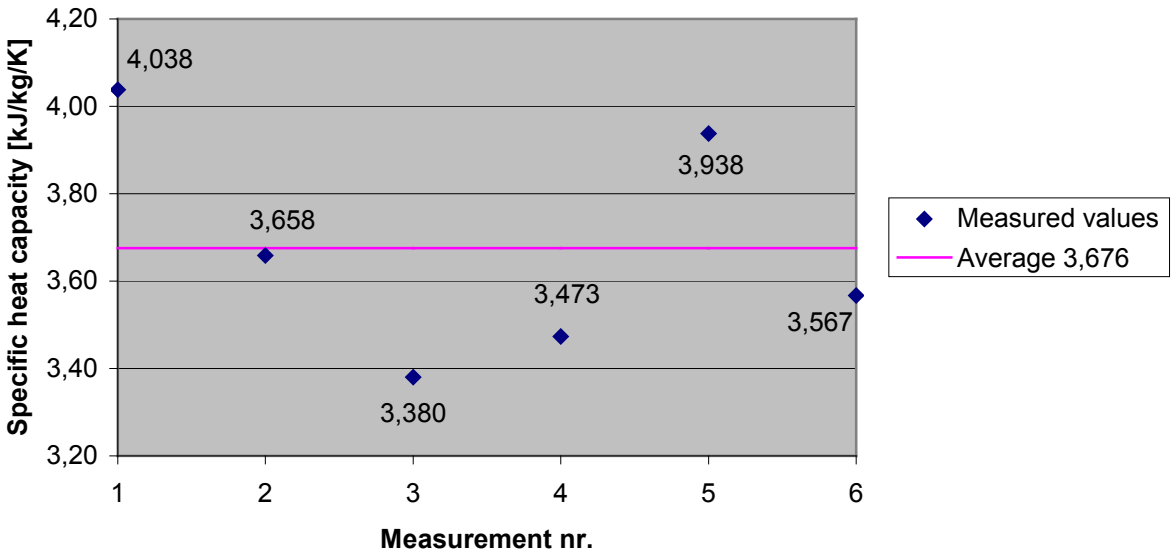

***Figure 32**: Specific heat capacity of dry water*

The values were found to be significantly lower than the theoretical calculated value in which the air content had not been considered. The average value of the specific heat capacity was determined to $c_{DW} = 3{,}676 \frac{kJ}{kgK}$ (see also Appendix V: Heat capacity).

As already the theoretical calculated heat capacity demonstrated, dry water shows similar to bulk water a particularly high value.

6.8. Droplet characterization

A high content of water in a stable powder formation suggests a good protective shell of silica particles which is apparently not too thick. Also a great number of droplets lead to a huge water/air interface with silica particles between.

Considering the dimension of one dry water droplet and given the global ratio of water in the system, it is possible to evaluate the amount of silica covering the droplet. An estimation of the number of droplets in a certain volume can be done in order to calculate the area of the water/air interface.

It is assumed that all silica particles are involved in the coating formation. The primary dry water particulates with an average diameter of D_p = 10 µm are considered as a sphere. The density of a dry water particulate is accepted to be the tapped density of ρ_{tapped} = 625,8 g/L specified in the chapter "6.6. Flowability". The surface area is calculated with the amount of dry water particles occurring in the bulk volume ρ_b = 570 g/L determined in chapter "6.3. Density".

6.8.1. Silica shell thickness

The particulate as seen in Figure 33 is characterized by a volume V_p of

$$V_p = \frac{4}{3} \cdot r^3 \cdot \pi = 524\ \mu m^3 \qquad (6.10)$$

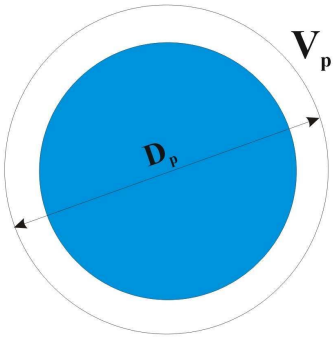

Figure 33: *Schematic of a dry water particulate*

The mass m_p of a particulate is therefore

$$m_p = \rho_{tapped} \cdot V_p = 3{,}28 \cdot 10^{-10}\ g \qquad (6.11)$$

From Equation (6.11) the mass of silica shell m_s can be calculated in consideration of the ratio of silica particles in the system of 10 % by weight.

$$m_s = 0{,}1 \cdot m_p = 3{,}28 \cdot 10^{-11}\ g \qquad (6.12)$$

Supposing that the density of the silica network is equal to the tapped density of fumed silica ρ_{fs} provided by the supplier, e.g. ρ_{fs} = 200 g/L, the volume of the shell can be determined to

$$V_s = \frac{m_s}{\rho_{fs}} = 164\ \mu m^3 \qquad (6.13)$$

The volume of the water droplet V_w inside the shell (Figure 34) is the difference between the volume of the whole particulate and the shell volume (Equation (6.14)).

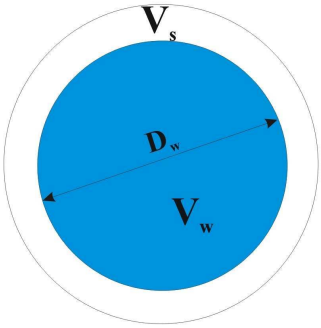

Figure 34: *Schematic of volumes*

$$V_w = V_p - V_s = 360\ \mu m^3 \qquad (6.14)$$

The diameter of the water droplet D_w can be calculated with Equation (6.10), the formula for spheres.

$$D_w = 2 \cdot r_w = 2 \cdot \sqrt[3]{\frac{3 \cdot V_w}{4 \cdot \pi}} = 8{,}8\ \mu m \qquad (6.15)$$

With Equation (6.15), the thickness of the corresponding silica envelope comes to approximately 0,6 µm. Regarding a droplet size of 100 µm with the same approach, the silica shell has a thickness of 6 µm.

The silica particles reveal a very thin layer compared to its enclosed water droplet diameter evidencing strong interactions between among themselves.

6.8.2. Surface area

Considering a bulk density of ρ_b = 570 g/L (chapter "6.3. Density") and a particle volume of V_p = 524 µm³ (from chapter "6.8.1. Silica shell thickness"), in 1 g dry water (V = 1,75 cm³) are $3{,}35 \cdot 10^9$ droplets. Each dry water particulate has an estimated water droplet with a diameter of D_w = 8,8 µm and thus a surface calculated as follows:

$$A_w = \pi \cdot D_w^2 = 243\ \mu m^2 \qquad (6.16)$$

Hence, the dry water powder reveals a total specific water surface of

$$A = 3{,}35 \cdot 10^9 \frac{1}{g} \cdot 243\ \mu m^2 = 0{,}814 \frac{m^2}{g}.$$

When the mean droplet size is assumed to be 100 µm, the thickness of the silica envelope comes to 6 µm and the specific surface to 0,105 $\frac{m^2}{g}$ with the same calculations. The droplet characterization has been carried out assuming total spherical dry water particulates. In fact not all of the powder consists of perfect shapes. But nevertheless, the calculation of the shell thickness evidences strong interactions between the silica particles at very fine layers. The surface area reveals a large aerated interface of water/air with silica particles between.

6.9. Recyclability of silica particles

Since a dissociation between the silica shell and the water droplets took place under strong mechanical stress as well as after some freezing/thawing periods, the reusability of the silica particles were investigated.

After the release of water from the system, it could be easily reached a new powder formation by remixing the substances under the same conditions. The only drawback might be a reduction of the water content due to facilitating evaporation.

Since the silica particles have a high heat resistance with a melting point of 1700°C (Günther, 2008; Wacker Chemie AG, 2006) a total water removal can be carried out by warming up the substances for example in an oven. A warm environment (>50 °C) and some stirring from time to time lead to a total water evaporation without impairing the characteristics of the silica particles. The pure particles can be reused afterwards for a new dry water composition.

7. Summary of experiments

In the laboratory study, dry water powders were prepared in different ratios and elementary characteristics were determined. Strong stirring conditions are required to obtain encapsulated water droplets whereby the water ratio plays a key role. Powder formation with HDK® H2000 used in this study can be achieved with a maximum water content of 95 % by weight. A larger water content leads to mousse formation whereas less water decreases the mean droplet sizes of dry water particulates up to 10 µm. The most adequate powder properties exhibited dry water with a water content of 90 % by weight.

Although the particulates show a slightly cohesiveness by attracting to each other, dry water is characterized by a good flowability and unexpectedly easy handling in spite of a high water content and a high compressibility.

The powder particulates consist of water droplets coated by a thin layer of hydrophobic silica particles which prevents the water from coalescence. The protective shell also reduces water evaporation and keeps the droplets separated even in frozen conditions maintaining a flowability at minus temperatures.

The silica shell can be destroyed by strong mechanical stress or several freezing/thawing periods. Whereas the fumed silica particles, not influenced negatively after a mixing process, can easily be reused for new preparations.

Dry water powder shows with respect to the large water content an expected high heat capacity of c = 3,676 $\frac{kJ}{kgK}$, which is slightly less than bulk water.

Small droplets, increasingly spherical shaped at decreasing sizes, reveal a high interface of water and air with silica particles between. Also the air content rises with decreasing droplet size.

The rate of mass loss due to freezing shows a slower freezing process or rather a lower freezing temperature compared to bulk water. The reason is assumed to be the small water droplet size. It can be presumed a change of the water structure due to

the particle/water or solid/liquid interface respectively. Since the water droplets are very small the whole water droplets could be part of a modified structure. Thus, it would be well worth continuing detailed investigations of the water structure by focusing on the chemical background.

8. Applications of dry water

Although dry water has been known since 1964, little attention was devoted to it since possible applications were not immediately obvious. The pharmaceutical company Degussa, applicant of the first patent on dry water, saw a potential use of encapsulated water droplets in cosmetics storing and supplying water when it is needed. In 2004, they resumed the idea in several products like moisturizing makeups, advertising to the public as "dry water for the skin" (Hasenzahl, 2005). The food industry took up the idea providing a liquid in the powder which acts as a carrier (Lankes, 2006).

But also a simple application as a cooling agent is well possible even in a frozen state at minus temperatures. A large water content enables a great heat absorbing capacity while small droplets contribute to a highly distributed water-gas interface. This might be a conceivable benefit in the cooling processes of hot gases as it is needed after combustions. It remains to be clarified in what extent dry water will scrub particles or corrosive gases from the flue gas deserving an own study.

The largest potential may lie in the gas storage application in the form of gas hydrates. The danger of methane storage and transport can be reduced due to stable hydrate formations. Allowing to store and stabilize very large amounts of volatile gases without permanently binding them may help to expand its use as a future energy source. Methane hydrates in dry water could be a convenient way for the use in vehicles powered by natural gas.

It might be conceivable a economic storage of gas which would otherwise be burned up in a free flame, for example associated gas which comes up from oil fields. Also collecting and transporting natural gas from stranded deposits might get viable with dry water powder.

Storing huge amounts of carbon dioxide in an efficient way could help to reduce the quantitatively largest greenhouse gas in the atmosphere which has been provided great attention in politics of some countries for quite some time now (Wuppertal Institut, 2007).

In the chemical industry dry water could also have a potential application. As a means to speed up catalyzed reactions between a gas and the encapsulated starting product without the need of stirring could benefit an effective large-scale production.

Dry emulsions can potentially offer a way of easier handling and transporting hazardous liquids and other harmful industrial materials since they become less or non-reactive when they get trapped. Thereby an inherent advantage of the dry water process is the transformation of substances from "splash-able" liquid into a "dry state" powder.

9. Conclusions

This thesis presented the unusual and largely unknown substance dry water. Since it is not well known yet, the work was focused on the basic information of how dry water occurs and what its generally properties are.

The water-rich powder containing encapsulated microscopic water droplets is a solidified form of water which is characterized by a good flowability. The protected droplets and its large water/air interface makes dry water to an unique substance which is simple to prepare and harmless to humans and the environment.

Even though the technical applications are not immediately obvious, the powder offers great chances for a number of uses. As an effective storage for large amounts of gases, a green catalysis medium or as a save storage medium for harmful materials - dry water could make big waves in the future.

But nevertheless, the substance is not applied in a large scale since it is not fully elucidated. It is well worth keeping dry water as an object of research. Applying dry water as a scrubbing agent in flue gases may deserve a specific study. On the one hand, the cohesiveness on the silica particles could contribute to an increased mechanical scrubbing of solid particles like soot from the flue gas. On the other hand, a simultaneous chemical separation of pollutants could be achieved by using the dry water method as dry acid. The so-called Walther-method for example implements a desulfurization and denitrification of flue gases using ammonia solution (Fritz, 1990). A dry ammonia solution may be a conceivable improvement for the process.

Also the chemical structure of the water droplets might conceal great scientific interests. The deviating freezing properties of dry water might suggest a difference of the structure, dynamic or chemical environment of the water molecules compared to bulk water. A NMR spectroscopy of dry water could be a technique for determining physical and chemical properties of the atoms and molecules.

If it is possible to expand its range of potential applications and to rise it to a marketable product, dry water could become a place in the modern world of sustainable energy materials.

References

Andersson, S. (1992). Thermal conductivity and heat capacity of amorphous SiO2: Pressure and volume dependence. *Journal of Physics.Condensed Matter, 4*, 6209.

Barry D. Allan. (1977). *Dry water - patent US400170A*

Berner, E. K., & Berner, R. A. (1987). *The global water cycle : Geochemistry and environment*. Englewood Cliffs, N.J.: Prentice-Hall.

Bigg, E. K. (1953). The supercooling of water. *Proceedings of the Physical Society.Section A, 66*, 688.

Binks, B. P., & Murakami, R. (2006). Phase inversion of particle-stabilized materials from foams to dry water. *Nature Materials, 5*(11), 865-869. doi:10.1038/nmat1757

Carlowitz, B. (1986). *Kunststofftabellen* (3, völlig überarb. u. erw. Aufl. ed.). München: Hanser.

Carter, B. O. (2010). Pausing a stir: Heterogeneous catalysis in "dry water". *Green Chemistry, 12*(5), 783-785.

Carter, B. (2010). Dry water: Making waves. *Chemistry and Industry,* (22), 22-24.

Carter, B. O., Wang, W., Adams, D. J., & Cooper, A. I. (2010). Gas storage in "dry water" and "dry gel" clathrates. *Langmuir : The ACS Journal of Surfaces and Colloids, 26*(5), 3186-3193. doi:10.1021/la903120p

Cullen, P. J. (2003). Rotational rheometry using complex geometries - A review. *Journal of Texture Studies, 34*(1), 1.

Demirbas, A. (2010). *Methane gas hydrate*

Devine, R. A. B. (2000). *Structure and imperfections in amorphous and crystalline silicon dioxide*. Chichester: Wiley.

Dr. Mathias Schulenburg. (2008). In Bundesministerium für Bildung und Forschung (BMBF) (Ed.), *Nanopartikel - kleine Dinge, grosse Wirkung*. Bonn, Berlin:

Forny, L. (2009). Influence of mixing characteristics for water encapsulation by self-assembling hydrophobic silica nanoparticles. *Powder Technology, 189*(2), 263.

Forny, L. (2011). Dry water: From physico-chemical aspects to process-related parameters.

Forny, L., Pezron, I., Saleh, K., Guigon, P., & Komunjer, L. (2007). Storing water in powder form by self-assembling hydrophobic silica nanoparticles. *Powder Technology, 171*(1), 15-24. doi:DOI: 10.1016/j.powtec.2006.09.006

Fritz, W. (1990). *Reinigung von abgasen: Gesetzgebung zum Emissionsschutz, Maßnahmen zur Verhütung von Emissionen mechanische, thermische, chemische und biologische Verfahren der Abgasreinigung Entschwefelung und Entstickung von Feuerungsabgasen. physikalische Grundlagen: Technische Realisierung*

Günther, T. (2008). *Zum Fällungsprozess und Wachstum kugelförmiger SiO2-Partikel.*

H. Kuno, M. S. (1967). Rheological behavior of powder in a rotational viscometer.

Hannink, R. H. J., & Hill, A. J. (2006). *Nanostructure control of materials* Woodhead Publishing.

Hasenzahl, S. (2005). Dry water for the skin. *SOÉFW-J., 131*, 1-8.

Kate White. (2005). *Ice engineering - engineering and design (EM 1110-2-1612)* U.S. Army Corps of Engineers.

Lankes, H. (2006). Liquid absorption capacity of carriers in the food technology. *Powder Technology, 134*(3), 201-209.

LfU BW. (Juli 2007). *Anwendung von Nanopartikeln*. Landesanstalt für Umwelt, Messungen und Naturschutz Baden-Württemberg;:

M. Sc. Hicham Ahmad Fadel. (2005). *Modifizierung von Kunststoffen mit Nanodomänen.* (Doctor rerum naturalium, Fachbereich Chemie der Technischen Universität Darmstadt).

R. Carr. (1965). Evaluating flow properties of solids. *Chemical Engineering, 18*

Roberts, M. W. (1997). *Interfacial science; international union of pure and applied chemistry*. Oxford: Blackwell Science.

Schulze, D., & SpringerLink. (2008). *Powders and bulk solids*. Berlin, Heidelberg: Springer-Verlag Berlin Heidelberg.

Schutte, D. Schmitz, F.-T. & Brünner, H. (1968). *Predominantly aqueous compositions in a fluffy powdery form approximating powdered solids behavior and process for forming same*

Skogsberg, K. (2005). *Seasonal snow storage for space and process cooling*

Sloan, E. D. (2003). Fundamental principles and applications of natural gas hydrates. *Nature, 426*(6964), 353-359.

VDI, & VDI-Verein Deutscher Ingenieure, Gesellschaft Verfahrenstechnik und Chemieingenieurwesen. (2010). *VDI heat atlas* [VDI-Wärmeatlas.] (2nd ed.). Heidelberg: Springer.

Wacker Chemie AG. (2006). *Safety data sheet (1907/2006/EC) for HDK®*

Wacker Chemie AG. (2009). *Product overview- HDK® pyrogenic silica*

Wacker Chemie AG. (2011). *Technical data sheet for HDK®H2000*

Wang, W., Bray, C. L., Adams, D. J., & Cooper, A. I. (2008). Methane storage in dry water gas hydrates. *Journal of the American Chemical Society, 130*(35), 11608-11609. doi:10.1021/ja8048173

WHO, I. (2010). *WHO classification of tumours of the digestive system*

Wuppertal Institut. (2007). *Geologische CO2-Speicherung als klimapolitische Handlungsoption.*

Appendix I: Density

Table 2: *Density and air content measurements and calculations*

	Water content					
	90 wt%		95 wt%		97 wt%	
	poured	shrunk	poured	shrunk	poured	shrunk
Mass [g]	90		85		87,85	
Volume [ml]	242	158	128	120	120	116
Density ρ [g/L]	**371,9**	**569,6**	**664,1**	**708,3**	**732,1**	**757,3**
Pure density ρ_0 [g/L] (without air)	1058		1028		1017	
Air content φ [vol%]	**64,8**	**46,1**	**35,4**	**31,1**	**28,0**	**25,5**

The mass and volume are measured values, the pure density and air content were calculated from the densities of water (ρ = 1000 g/L) and silicon dioxide (ρ = 2200 g/L). The air content were determined with Equation (5.4)(page 30):

$$\varphi = (1 - \frac{\rho}{\rho_0}) \cdot 100$$

The pure density ρ_0 can be calculated from the theoretical pure volume of dry water (V_{DW0}), the water volume (V_w)and the particle volume (V_p).

$$V_{DW0} = V_W + V_p \qquad (11.1)$$

$$\frac{m_{DW0}}{\rho_0} = \frac{m_w}{\rho_w} + \frac{m_p}{\rho_p} \qquad (11.2)$$

$$\rho_0 = \frac{m_{DW0}}{\frac{m_w}{\rho_w} + \frac{m_p}{\rho_p}} \qquad (11.3)$$

The masses m_w and m_p can be written as a function of m_{DW0} depending on the water mass fraction ω. They are in the following relation to each other:

$$m_{DW0} = 1 \qquad (11.4)$$

$$m_W = \omega \cdot m_{DW0} \qquad (11.5)$$

$$m_p = (1 - \omega) \cdot m_{DW0} \qquad (11.6)$$

Thus, the equation for the pure density ρ_0 is

$$\rho_0 = \frac{1}{\frac{\omega}{\rho_w} + \frac{1 - \omega}{\rho_p}} \qquad (11.7)$$

Appendix II: Viscosity

Table 3: *Viscosity measurement with viscometer Visco Star - L*

Rotational speed [rpm]	**Viscosity [mPas]**	
	Spindle L3	Spindle L4
200	230	180
100	540	400
60	980	680
50	1280	940
30	2770	2000
20	4000	3200
12	7600	5800
10	8900	8000
6	15300	10400
5		17400

With the spindle L3 at a rotational speed of 5 rpm, the measuring range was exceeded and therefore no representative value was maintained.

Appendix III: Mass loss due to freezing

Table 4: *Mass loss measurement with pure water*

	Freezing (-20°C)		Cooling (+5°C)	
Time [h]	**Mass [g]**	**Mass loss [g]**	**Mass [g]**	**Mass loss [g]**
0	27,586	0	27,135	0
0,5	27,230	0,356	26,923	0,212
1,0	27,053	0,533	26,746	0,389
1,5	27,008	0,578	26,587	0,548
2,0	27,000	0,586	26,439	0,696
2,5	26,994	0,592	26,314	0,821

Table 5: *Mass loss measurement with dry water*

	Freezing (-20°C)		Cooling (+5°C)	
Time [h]	**Mass [g]**	**Mass loss [g]**	**Mass [g]**	**Mass loss [g]**
0	19,933	0	18,464	0
1	19,781	0,152	18,284	0,180
2	19,744	0,189	18,223	0,241
3	10,727	0,206	18,180	0,284
4	19,516	0,211	17,873	0,307

Appendix IV: Evaporation rate

Table 6: *Dry water mass decrease with 90 wt% water content*

Days	Dry water [g]	Water decrease from beginning [g]
0	85,67	0
1	76,14	9,53
2	71,12	14,55
4	62,42	23,25
7	49,10	36,57

Table 7: *Dry water mass decrease with 95 wt% water content*

Days	Dry water [g]	Water decrease from beginning [g]
0	91,99	0
1	80,12	11,87
2	73,63	18,87
4	62,79	29,20
7	46,31	45,68

Table 8: *Dry water mass decrease with 97 wt% water content*

Days	Dry water [g]	Decrease from beginning [g]
0	91,78	0
1	77,05	18,73
2	67,14	32,64
4	52,26	49,52
7	31,91	62,87

Table 9: *Mass decrease with bulk water*

Days	Dry water [g]	Decrease from beginning [g]
0	148,78	0
1	124,57	24,21
2	101,92	46,86
4	63,47	85,31
7	2,64	146,14

Appendix V: Heat capacity

Table 10: *Heat capacity measurements 1 - 3*

Measurement Nr.	**1**		**2**		**3**	
Plastic bag [g]	2,118		2,091		2,079	
Cut off [g]	1,427		1,26		1,66	
Plastic [g]	0,691		0,831		0,419	
Plastic bag with DW [g]	19,406		11,735		6,594	
	Water	**DW**	**Water**	**DW**	**Water**	**DW**
Temperature [°C]	47,1	21,4	46,8	21,4	47,8	21,4
Mass [g]	139,8	18,715	105,68	11,735	109,92	6,594
Final temperature [°C]	44,1		44,6		46,6	
Spec. heat cap. [kJ/kg/K]	4,038		3,658		3,380	

Table 11: *Heat capacity measurements 4 - 6*

Measurement Nr.	**4**		**5**		**6**	
Plastic bag [g]	2,078		2,076		2,061	
Cut off [g]	1,694		1,433		1,457	
Plastic [g]	0,384		0,643		0,604	
Plastic bag with DW [g]	7,857		8,518		6,550	
	Water	**DW**	**Water**	**DW**	**Water**	**DW**
Temperature [°C]	44,6	21,4	50,9	21,4	49,6	21,4
Mass [g]	100,15	7,857	107,09	8,518	121,98	6,550
Final temperature [°C]	43,2		48,9		48,4	
Spec. heat cap. [kJ/kg/K]	3,473		3,938		3,567	